KEY LECTURES

KL-01
FROM GUM ELASTOMERS TO FILLED VULCANIZED RUBBER: RHEOLOGICAL MODELING OF THE NON-LINEAR BEHAVIOR

FABIO BACCHELLI, and SALVATORE COPPOLA

ENI - POLIMERI EUROPA, Centro Ricerche Elastomeri
via Baiona 107, 48100 Ravenna, Italy,
fabio.bacchelli@polimerieuropa.com

Processing of rubber compounds involves the application of rapid and large deformations in both shear and elongation. This indicates that transient flow and a large degree of stretching are actually prevalent. Nevertheless, the analysis of unit operations is usually performed on the basis of the rheological response to steady state, mild shear flow. Moreover, commonly used constitutive equations for rubber elasticity do not point out the contribution of the raw elastomer in the vulcanizate response.

Commercial rubbers possess more complex structures with respect to model polymers and the non-linear rheology of a compound is strongly affected by changes in the relaxation time spectrum of its polymer matrix as a consequence of variations in molar mass distribution or branching patterns, together with filler loading and filler dispersion.

Up to now, there is a lack of a comprehensive theory, which can simultaneously describe the rheology of the raw elastomer, the response of filled rubber and its behavior in the final cured state. Then, the problem of describing and modeling the nonlinear behavior of rubber at different processing stages should be approached by collecting various theoretical and experimental contributions.

The non-linear behavior of the polymer matrix can be described using micro-rheological models accounting for reptation together with the contribution of chain stretch and dissipative convective constraint release. The time-dependent response of the filled polymer with a particle loading above the percolation threshold can be approached by introducing terms describing the filler-polymer dynamics under flow. Rheological modeling can be extended to the post-cure state to describe Mullins stress-softening-hysteresis and other aspect of the vulcanizate with a very limited number of parameters.

A commercial high-*cis*-polybutadiene (*cis*-BR) was investigated in the present work (Neocis BR40, Polimeri Europa), characterized by a 1,4-*cis* content of 97 %. The polymer, nearly linear, has an average molecular weight of 420 000 g mol^{-1} and a polydispersity index of 3.8. Carbon black compounds (N990, N330) were prepared in a Brabender Plasticorder with a filler volume fraction of 0.2. A Rheometric Scientific ARES A11 was used to determine the dynamic properties of *cis*-BR and related cured and uncured compounds.

Elongational measurements on cured and uncured rubber were performed with a detachable commercial fixture for rotational rheometers, which incorporates dual wind-up drums

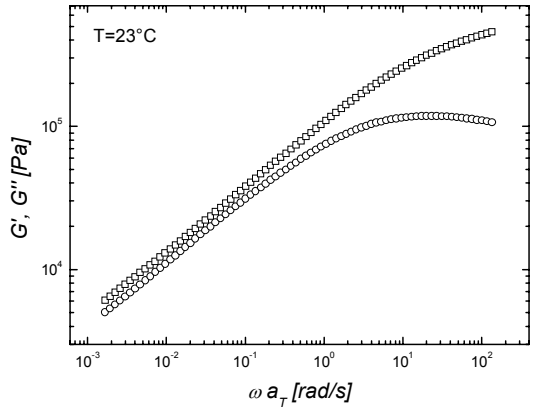

Fig. 1. **Linear viscoelastic data of a nearly linear *cis*-BR at 23 °C**

to ensure a truly uniform extensional deformation during uniaxial extension. A SER-HV-P01 (ref.[7]) platform was hosted by a Anton Parr Physica MCR 501. Uncured cylindrical specimens with an effective length of 12.7 mm were prepared by means of a Göttfert Rheograph 6000 capillary rheometer and relaxed for at least three days. Flat specimens were used for vulcanized rubber.

The linear viscoelastic behavior of a typical high-*cis*-BR is reported in Fig. 1. The crossover point was not observed in the investigated frequency range, accounting for the presence

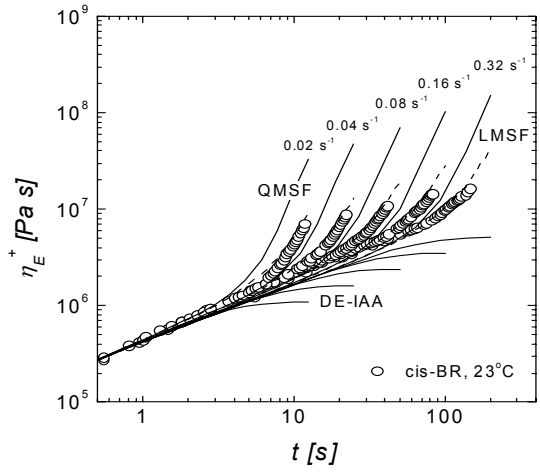

Fig. 2. **Startup flow of a nearly linear *cis*-BR in uniaxial extension at 23 °C.** Lines represent the linear (LMSF) and quadratic (QMSF) form of the Molecular Stress Function theory and the prediction of the Doi-Edwards theory under the assumption of independent alignment (DE-IAA)

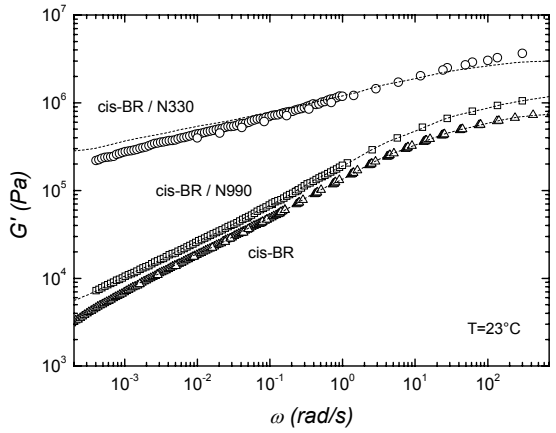

Fig. 3. **Elastic modulus of *cis*-BR and related carbon black compounds at 23 °C.** Dashed lines represent the model prediction

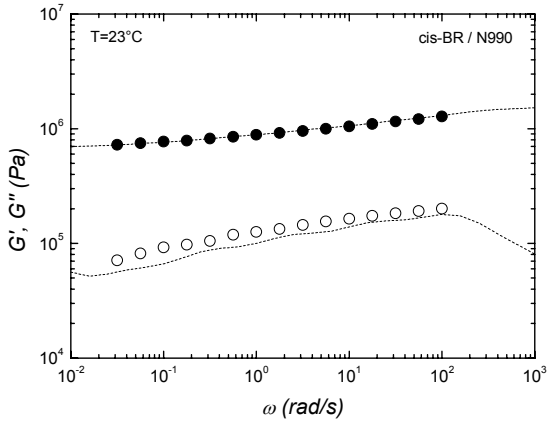

Fig. 5. **Dynamic moduli of vulcanized carbon black filled *cis*-BR (N990) at 23 °C.** Dashed lines represent the model prediction

of very long relaxation dynamics affecting many important processing parameters.

Data were used to access micro-rheological models for the prediction of the nonlinear response to different kinds of deformation. These models prove essential for understanding, for example, the important contribution of the strain hardening associated with the elongation of the polymer matrix in a compound. The extensional behavior of *cis*-BR at room temperature is reported in Fig. 2 for different Hencky strain rates.

Data are compared with the model known as Molecular Stress Function, accounting for reptation together with the contribution of chain stretch. An extended version of this generalized tube model with strain-dependent tube diameter was considered, to include the CCR contribution[3,5]. The prediction of the Doi-Edwards theory based on pure orientational contribution is also reported[4].

Industrial filled polymer compounds represent highly concentrated suspensions with complex interactions between filler particles and the polymer. Unlike the concentrated suspensions with low viscosity matrices the rheological behavior of rubber compounds can be described in terms of a single medium approach, though with complicated properties, because the high viscosities of the polymer matrices make the typical two-phase effects, such as internal rotations of the particles, presumably insignificant.

In comparison with the rheology of polymer melts and solutions, filled polymers display very long relaxation phenomena which reflect the processes of structurization (flocculation and aggregation) of particles in the medium.

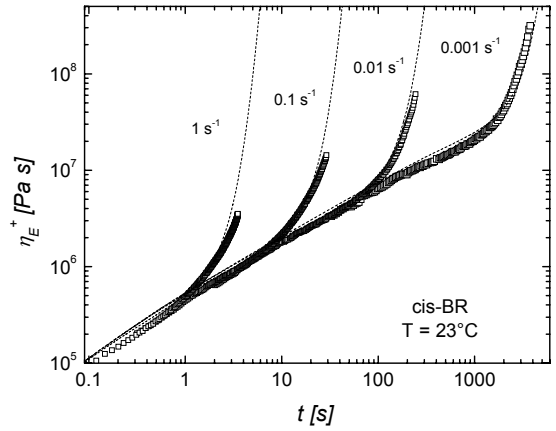

Fig. 4. **Startup flow of *cis*-BR in uniaxial extension at 23 °C and Hencky strain rates of 1, 0.1, 0.01 and 0.001 s^{-1}.** Lines represent the prediction of the Leonov's model

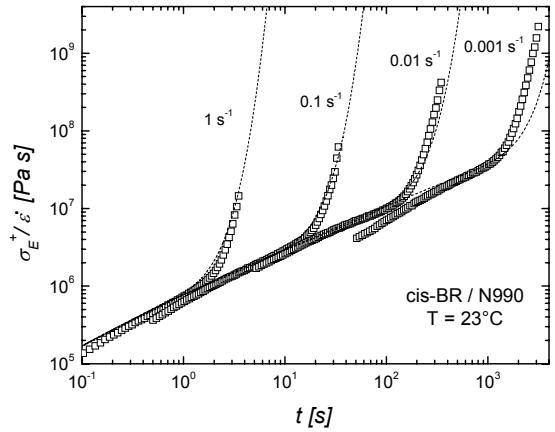

Fig. 6. **Startup flow of carbon black filled *cis*-BR in uniaxial extension at 23 °C and Hencky strain rates of 1, 0.1, 0.01 and 0.001 s^{-1}.** Lines represent the prediction of the Leonov's model

Tube models are not suitable for describing the relaxation dynamics of filled, uncured rubbers. Also the typical continuum mechanics approach commonly used for the modeling of polymer melts (K-BKZ, rubber-like liquid[2]) results largely unsatisfactory.

A set of thermodynamically consistent and stable constitutive/kinetic equations was proposed by Leonov and coworkers[1,6] to describe manifestations of particle-matrix interactions and polymer viscoelasticity.

Though not being a first-principles theoretical approach, the Leonov's model proves valid in describing almost the whole phenomenology of polymer nonlinear viscoelastic behavior. The model is based on two tensorial differential equations accounting for the stress carried by the free and trapped chains, respectively. A scalar kinetic equation is also necessary to describe the process of bonding/debonding of the polymer chains on the filler particles. Besides a discrete spectrum of relaxation times for the linear Viscoelastic behavior, the model just needs the determination of 4 parameters, two of them for describing the nonlinear viscoelasticity and two structural/kinetic parameters for the filler-matrix interaction.

Fig. 3 shows the dynamic elastic modulus for *cis*-BR and related uncured carbon black compounds. As expected, a significant effect of the different filler surface area (N330>N990) is observed in terms of linear Viscoelastic response for these compounds with the same filler loading. The linear Viscoelastic spectrum is extracted for each material from dynamic moduli. With an appropriate choice of the parameters for the nonlinear viscoelasticity, the strain hardening behavior in uniaxial extensional flow start-up is very well described for the pure polymer (Fig. 4). A similar procedure has been applied to the uncured compounds and to the vulcanized rubber (Fig. 5).

The Leonov's model predictions for filled uncured compounds were successfully compared with experimental data in in Fig. 6.

The application of the Leonov's model to the vulcanized compound is reported in Fig. 7, 8 in terms of Mullins stress-softening-hysteresis measured at constant Hencky strain rate. The model is able to predict the thixotropy effects of cyclic extensional deformations and results are in satisfactory agreement with model predictions. Interestingly, the Mullins effect predicted by the Leonov's model is reduced with respect to the experimental data. This suggests that filler-filler interactions, not modeled by Leonov's approach, cannot be fully neglected for these *cis*-BR/CB compounds.

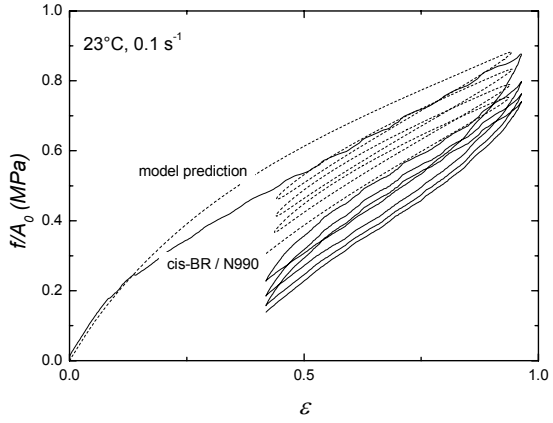

Fig. 7. **Mullins stress-softening-hysteresis of vulcanized carbon black filled *cis*-BR (N330) at 23 °C and |Hencky strain rate of 0.1 s^{-1}.** Dashed lines represent the Leonov's model prediction

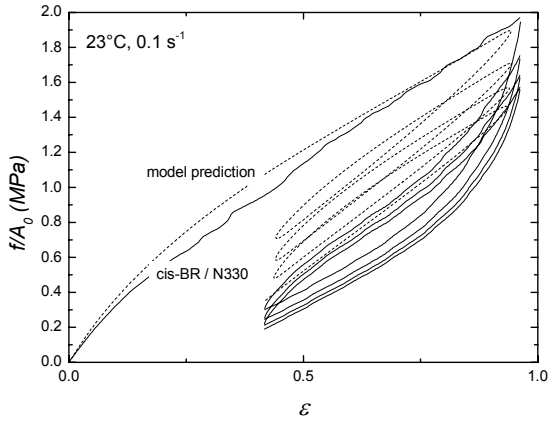

Fig. 8. **Mullins stress-softening-hysteresis of vulcanized carbon black filled *cis*-BR (N990) at 23 °C and |Hencky strain rate of 0.1 s^{-1}.** Dashed lines represent the Leonov's model prediction

The approach presented in this paper could be extended for capturing a wide range of rheological behavior of filled elastomers in a wide range of stresses and strain rates, for the description of various unit operation in rubber processing.

REFERENCES

1. Joshi G. P., Leonov A. I.: Rheol. Acta *40*, 350 (2001).
2. Larson R. G., in: *Constitutive Equations for Polymer Melts and Solutions*. Butterworth, Boston 1988.
3. Wagner M. H., Rubio P., Bastian H.: J. Rheol. *45*, 1387 (2001).
4. Doi M. Edwards S., in: *The Theory of Polymer Dynamics*, Oxford Science Publications, 1986.
5. Ianniruberto G., Marrucci G.: J. Non-Newtonian Fluid Mech. *65*, 241 (1996).
6. Leonov A. I.: J. Rheol. *34*, 1039 (1990).
7. Sentmanat M. L.: Rheol. Acta *43*, 657 (2004).

KL-02
AUTOMOTIVE APPLICATIONS OF THERMOPLASTIC ELASTOMERS

JIŘÍ GEORGE DROBNY

Drobny Polymer Associates
Merrimack, NH 03054 USA

Thermoplastic elastomers (TPEs) are rubbery materials with fabrication characteristics of conventional thermoplastics and many performance properties of thermoset (vulcanized) rubber. TPEs can be processed by the same methods such as injection molding, extrusion, blow molding, rotational molding, thermoforming as most thermoplastic materials, including polyethylene, polypropylene, and polyvinyl chloride. On the other hand, their basic properties are very similar to those of vulcanized rubber materials based on natural rubber, SBR, EPDM, NBR, and polychloroprene. Thermoplastic elastomers offer a variety of practical advantages over vulcanized rubber, such as simple processing with fewer steps, shorter fabrication times, and the possibility of recycling of production and post-consumer scrap. These and other advantages are the main reasons why the applications of TPEs in the automotive industry have been growing at a constantly increasing rate during the past two decades and currently automotive applications represent the largest single market for these materials. This contribution will discuss properties of the thermoplastic elastomers that are widely used in automobiles and their specific applications as well as the most recent developments.

The author of this contribution is an international consultant and university educator. His book “Handbook of Thermoplastic Elastomers” was published by Plastics Design Library/William Andrew Publishing in 2007.

KL-03
RUBBER REINFORCEMENT BY CARBON NANOTUBES BETWEEN MYTH AND REALITY

N. DURENT, M. OWCZAREK, and B. HAIDAR

Institut de Chimie des Surfaces et Interfaces, ICSI-CNRS UPR 9069, Université de Haute Alsace, Mulhouse, France
b.haidar@uha.fr

Carbon nanotubes have attracted much attention for their unique structure, as well as for their excellent mechanical, electrical and thermal properties. Most properties of carbon nanotubes are closely related with its anisotropic structure, their form factor and their nano-scale size are critical for understanding their behavior in solutions as well as in polymer composites. However, in the case of polymer-based composites, polymer/solid interactions, rubber adsorption, chain conformation… are just a few of numerous factors affecting the development of the interphase which controls the overall macroscopic behavior of such materials. Polymer-carbon nanotube, NTC's, blends are no exception of this frame but with an additional specific factor that has to be considered. In fact, when the scale of the solid surface approaches the scale of a polymer chain, or its segment, the opportunity of an efficient adsorption ought to be different from those identified on quasi-infinite even surfaces. Only when the length of the chains is significantly smaller than the tub radius, the curved surface is approximately even on a local scale so that the concept for flat surfaces can be applied. However, such considerations should not apply for significantly curved nanotube surfaces.

Stable physisorption, at a given temperature, is known to be achieved thanks to a high number of weak physical adsorption sites. Such mechanism is conceivable with even surfaces, or any surface considered as such. The establishment of stable polymer-nanotube links depends also on the number of interaction sites between the two partners that depends, on its turn, essentially on the polymer chain conformation. The goal of this work is to tempt an experimental measurement of the adsorption enthalpy on NTC's of macromolecules with variable natures and sizes, MW's.

In the present work three series of a commercial PDMS with different and distributed molecular weights (MW in the 4000 to 420 000 g mol^{-1} range), a polybutadiene, PB, of different molecular weights (in the 3,000 to 120,000 g mol^{-1} range) but of identical microstructure (1,2-PB content equal to about 80 %) and a polyethylene HDPE with different Melt Flow Index were selected. The chosen CNT's belong to the multi-walls carbon nanotubes family were purchased from Nanocyl (France). Rubbers adsorption measurements were performed from solution a flow micro calorimetric technique, FMC. Adsorption can be monitored by the determination of the amount of adsorbed polymer and the measurement of its heat (enthalpy) of adsorption.

Results show that for linear amorphous polymer adsorption takes place exclusively in a relatively small window of MW's; adsorption, in this case, is permanent and associated with a substantial amount of heat. Outside this window, adsorption is reversible and heat exchange is low. High MW's molecules do not adsorb presumably because of their failure to wind around the nanotube and low MW's because of their incapacity to yield a sufficient number of adsorption contact-points to insure permanent adhesion and to overcome thermal agitation, kT. Only intermediate MW's are short enough to be unfolded over the surface without too much entropic penalty but with enthalpic gain which still high enough to link these intermediate chains permanently to the nanotube surface. Semi-crystalline polymers adsorption on NTC's was found to depend on the same molecular forces, the adsorption stability in this case, however, is achieved by adsorption nucleating crystal growth and the formation of the so-called nano hybrid “shish-kebab”.

Results are discussed in term of entropic penalty, enthalpic gain, polymer to tube scale-matching and radius of curvature of the NTC's surfaces.

KL-04

POWDER INJECTION MOULDING FOR AUTOMOTIVE APPLICATIONS - AN ALTERNATIVE TO TRADITIONAL PROCESSING ROUTES

BERENIKA HAUSNEROVÁ

Polymer Centre, Faculty of Technology, Tomas Bata University in Zlin, TGM 275, 762 72 Zlin, Czech Republic
hausnerova@ft.utb.cz

The possibility to use a forming method for plastics – injection moulding – to produce metallic and ceramic parts is still not widely spread information within polymer processing society.

Powder Injection Moulding (PIM) technology is a state of art process allowing the large-number production of relatively small parts of complex shapes with reduced cost and increased efficiency by avoiding the use of extra processes comparing to traditional metallurgical processes as machining or investment casting.

During the process (Fig. 1), powder is mixed with suitable polymers (called binder) into a homogeneous compound. In the next step, compound in the form of granules is formed in conventional injection moulding machines for thermoplastics into the final shape. This stage is followed by debinding, where the binder is extracted from the green part. Finally, compact is sintered so as to obtain the final part, which is purely metallic (Metal Injection Moulded – MIM) or ceramic (Ceramic Injection Moulded – CIM).

PIM process concerns several steps, and therefore the number of process variables is very high and their interactions are only partially understood. In this presentation, the important factors of the particular steps to the successful PIM processing will be briefly discussed.

Step 1: Mixing. During mixing the powder selected for the particular application is mixed together with a suitable polymer binder. Binder has usually a multicomponent character for the two reasons: good adhesion to powder at reasonable price during moulding, and different decomposition temperatures or chemical stability of its components during debinding.

Thermoplastics based binders predominate, but usage of thermosets, water based and gellation systems have been also

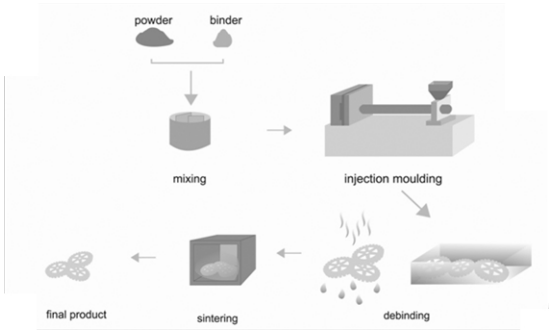

Fig. 1. **PIM processing steps**

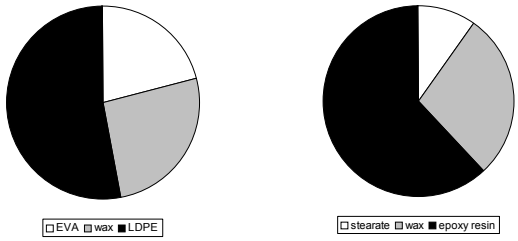

Fig. 2. **Examples of polymer binder compositions**

reported[1]; for examples see Fig. 2. The major part of a thermoplastic binder is typically low molecular weight polymer – a wax. However, due to its low viscosity, the shear forces necessary to disperse the particles and break up agglomerates may not be sufficient.

Additionally, as a consequence of the non-polar character, wax (when used alone) tends to migrate from the feedstock during moulding due to its poor adhesion to powder as we have demonstrated for cemented carbides compounds[2].

The other binder components, containing higher-molecular-weight polymers and additives, should provide suitable interactions with powder, and thus prevent the separation from powder during the flow. Block copolymers are often used for this purpose since they can be made of polymer blocks soluble in the dispersion medium and blocks with high affinity to powder imparting steric stabilisation of a compound. When we compared three types of polymer binders differing in the block copolymer used[3] (ethylene-butyl acrylate, ethylene-vinyl acetate, ethylene-acrylic acid) the influence of the flow properties of the particular binder composition diminished as the volume concentration of a solid component increased to 30 vol. %.

Mixing is carried out under high shear forces in order to break up agglomerates and disperse polymer binder efficiently on the powder surface as demonstrated in Fig. 3.

The crucial point during mixing is an adjustment of optimal loading (powder-binder ratio). Optimal loading refers[4] to powder concentration for which compound exhibits good flow properties (viscosity less than 10^3 Pa s) as well as homogeneity and stability in the shear rate range from 10^2 to 10^5 s^{-1}. It occurs slightly below a maximum (critical) packing fraction

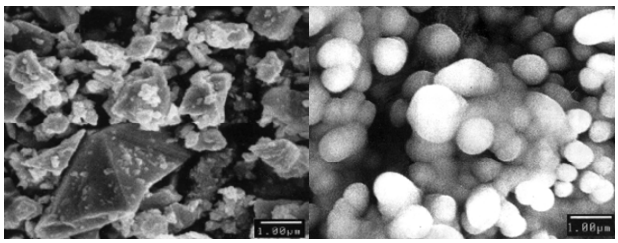

Fig. 3. **SEM of pure carbide powder and carbide powder-based PIM compound**

attainable for a given system; according to Dihoru et al.[4] it should be set 6–14 % lower than the maximum value.

In order to obtain maximum packing fraction for the particular powder/binder system, relative viscosity (ratio of the mixture viscosity to the viscosity of pure polymer) as a function of volume fraction of solids is often employed. The method is based on the assumption that powder particles stay mobile only to some filling degree (a cluster model). As the particles loading reaches the maximum a melt is confined among powder particles and the motion of the compound is made impossible, which results in a sharp increase of viscosity beyond all limits due to the friction between small hard powder particles[5].

The value of the maximum packing fraction depends strongly not only on the materials properties, but also on the packing conditions. Nielsen[6] proposed that the value of maximum packing ranges from 0.601 to 0.637 for random packed spheres, Chong et al.[7] used the value 0.605 for monodispersed glass beads in PIB matrix, e.t.c.

More than hundred empirical and theoretical relations have been proposed in order to obtain the value of maximum packing fraction from the viscosity data. Often a simple empirical Maron-Pierce relation[8] is employed to calculate maximum loading level for PIM compounds. In cases, where the Maron-Pierce model departs from experimental data, as shown e.g. by Jorge et al.[9] for the description of alumina powder and PEG/PE wax binder, its modification proposed by German and Bose[1] offers the good accordance with experimental data, predicting the maximum loading degree value with high accuracy.

Recently, we tested[10] a set of most often recommended relations in the PIM literature and found that the values predicted with the models were rather overestimated or underestimated, when compared to the experimental data. Further, the predicted values of the maximum volume fraction of the same powder varied with the model used (Table I) even though the maximum loading levels of PIM compounds, established using these models, followed well the powder characteristics: the highest value of maximum loading belonged to the powder with the broadest distribution of particle sizes, while the lowest value was attained for powder with high portion of small particles.

Table I
Predicted values of maximum volume fraction of solids for three carbide powders (UNI 1, UNI 2, BI) differing in their powder characteristics[10]

Model	Maximum volume fraction of powder, ϕ_m		
	UNI 1	UNI 2	BI
Eilers	0.60	0.56	0.63
Chong	0.60	0.56	0.62
Fedors	0.68	0.60	0.70
Frankel-Acrivos	0.60	0.53	0.61
Quemada	0.64	0.58	0.66
Graham	0.58	0.53	0.59
Krieger - Dougherty	0.66	0.57	0.59
Sengun - Probstein	0.71	0.70	0.61

Another rheological method to obtain critical powder volume concentrations has been proposed by Barreiros and Vieira[11], which employed torque rheometry to set optimal compositions of feedstocks based on powders having non-conventional characteristics for PIM. The optimal particle loading was evaluated as the highest value resulting from the intersections of the adjustment of linear functions of the mixing torque as a function of powder loading plots. The product coming from the feedstock selected by this method showed high density and flexural strength.

Recently, Dihoru et al.[4] demonstrated a possibility to determine optimal solid loading by the help of neutral network modeling. Consequently, they proposed an idea of combining neural networks with knowledge-based systems to optimize PIM process.

It should be mentioned that volume fraction of particles also slightly varies due to pressurization, because of a great discrepancy between bulk moduli of powder and binder[5]. Except of the pressure affected flow behaviour of PIM compounds reported by Hausnerova et al.[12] for the system consisting carbide powder and three-component binder (polyethylene, polyethylene based copolymer, paraffin wax), the effect of pressure is still omitted in the rheological characterization of filled polymers.

Step 2: Injection Moulding. Moulding of PIM compounds does not essentially vary from the processing of pure polymer melts. Both the screws and the barrels should be made from a wear resistant material. The screws are equipped with a non-return valve[13], which prevents feedstock's pressing backwards into the barrel.

Temperature is the most important variable – too high temperature can lead into the binder separation from the melted compound, on the other hand insufficiently high temperature would cause freezing of the feedstock before the mould filling or creation of weld lines. Computer aided engineering (CAE) gives the predictions of pressure, velocity and temperature profiles throughout the flow region via commercially available PIMSolver (Cetatech, South Korea), which is a 2.5D FEM software package developed for the simulation of the injection moulding process[14].

Nevertheless, a key to successful injection moulding lies in understanding of their rheological properties. A priori application of the fundamental theories on the suspensions in predicting the flow properties of PIM compounds should be taken with an extreme caution, because it brings a number of obstacles and limitations.

The rheology of such an extreme type of filled polymers has been documented in a far from sufficient manner. Majority of researchers concentrated on the effect of binder composition on rheological properties of feedstocks, but the role of the particular binder components and their interrelationship remain still unclear. One of the rare systematic investigations has been presented by Hsu and Lo[15]. They used McLean-Anderson statistic method[16] to study fluidity (inverse of viscosity) and pseudoplasticity (in terms of power-law index) of 15 binder formulations and presented contour maps showing how these two rheological variables vary with binder components at a constant value of the fourth.

PIM compounds generally show high sensitivity to variations in shear rate. Newtonian plateau becomes reduced or even disappear in the measured range of shear rates. It has been widely accepted that the change into non-Newtonian flow arises from the disruption of agglomerates formed by particles[17].

Depending on the type of the dispersed particles, especially on their particle size, yield point may appear for highly concentrated compounds at low shear rate as an indication of particle network structure within the melt, which is relatively stable at lower shear rates, e.g.[18]. At higher shear rates, however, this structure is broken, and the viscosity is dominated by hydrodynamic interactions[19] resulting in shear thinning as particles and polymer orientate and order in the flow direction to allow interparticle motion.

At still higher powder loading, with further rise of shear rate, volume increases because particles cannot form layers and slide over each other[20]. Then, depending on the binder wetting characteristics, shear thinning may turn into dilatant flow, as shown in Fig. 4.

There is still considerable uncertainty about the source of such behaviour. An increase in viscosity with shear rate may be indicative of particle disordering[20] or dilation.

The mechanism proposed by Barnes[21] is that with increasing shear stress (rate) the layers formed in the pseudoplastic flow region becomes disrupted, and at a certain (critical) shear stress or rate are fully eliminated and the flow turns into dilatant. It implies that each highly concentrated suspension exhibits dilatant flow at the proper flow conditions depending on filler concentration, particle size distribution, and also viscosity of a polymer component.

Finally, highly concentrated compounds (about 50 vol.% solids and higher) may exhibit a radical change on their flow curves accompanied by distortions of the extrudate surface called melt flow instabilities. Hausnerova and coworkers[2,22] recorded flow instabilities of a "pressure oscillations" type for carbide compounds and showed that temperature is the key factor limiting their onset almost independently of the filler concentration. At higher temperatures the formation and reformation of particles mat at the capillary entrance is enhanced by lower binder viscosity, which supports the mechanism of filtration effect, as a possible explanation.

Phenomenon considered as typical to occur during flow of highly concentrated suspensions is wall slip. Mooney method is a common approach to detect presence of wall slip during rheological measurements. The later approach to evaluate wall slip given by Hatzikiriakos and Dealy[23] is based on the slip velocity dependence on the wall normal stress.

For cemented carbides in a three-component binder (PEG, PMMA, stearic acid) the existence of a crisscross slip has been reported by Chunkrerkkul et al[24]. It is phenomenon occurring typically for clays in water, where the flow occurs on sets of slip bands (mobile binder) formed on planes near to the planes of maximum shear tress. The slip bands are composed of aligned particles layers of a plate shape, which slip one past another, lubricated by water. The authors propose a "slip band model" resulting in equation similar to the empirical relations of Maron-Pierce[8] or German and Bose[1] bearing relative viscosity to the volume fraction of filler.

Step 3: Debinding. Debinding is the most time consuming stage, depending mainly on the compact thickness and binder composition. A typical wall thickness of a PIM parts ranges from 2 to 3 mm, generally down to 0.1 mm (ref.[25]).

The binder has to be extracted from the pores as a fluid without distorting or contaminating the compact. There are two general ways of debinding (Fig. 5) – thermal and solvent, which are often combined in order to accelerate the process[1]. The first one proceeds by degradation and evaporation or liquid extraction. Thermal debinding in gaseous form is run under low (diffusion) or high pressure (permeation). Liquid extraction is carried out at a temperature high enough for the binder to reach sufficiently low viscosity to flow out of the compact into the pores of the wick material. The other type of debinding, solvent debinding, involves immersing the compact in a fluid that selectively dissolves some components of the polymer binder, thereby leaving an open pore structure for subsequent debinding by evaporation[5].

In general, thermal debinding should be carried out by sequential diffusion of the binder components, and therefore the binder should consist of at least two components with different diffusion temperatures.

In Fig. 6 thermogravimetric analysis of a paraffin wax is shown[2]. Debinding time increases with the chain length and paraffin wax has only between 18 and 32 carbon atoms; it has a narrow decomposition range (Fig. 6a). In contrast, binder containing components differing in molecular weights, melting and decomposition temperatures facilitates a step-by-step debinding. As it is evident from the results shown in Fig. 6b, PEG and paraffin wax move (by diffusion and viscous flow) to the surface of the part before PE and EVA, creating pores which enable easier evaporation of the rest of the binder[2].

Step 4: Sintering. The demands on PIM powders during moulding, debinding and sintering are contradictory. Small particles allow faster sintering, but on the other hand increase

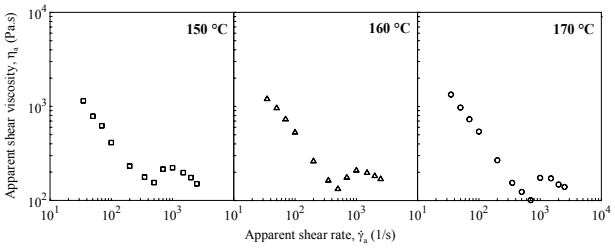

Fig. 4. **Flow curves of ceramic compound at various temperatures**

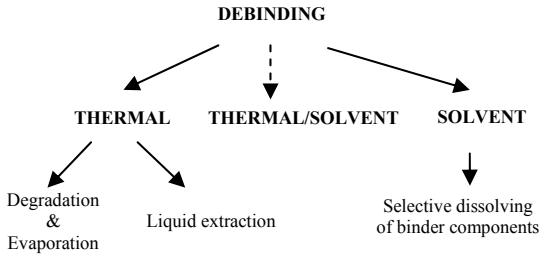

Fig. 5. **Schema of debinding techniques**

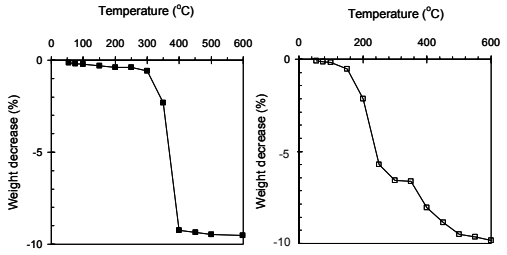

Fig. 6. **Thermo-gravimetric analysis of binders containing;** (a) paraffin and (b) paraffin, PE, PEG 6000, and EVA copolymer[2]

sintering shrinkage, give slower debinding compared to larger particles, and are considerably more expensive. A broad particle size distribution offers higher packing density, less sintering shrinkage, but it causes slower debinding[26]. The disadvantages of spherical particles are slumping during debinding and lower compact strength[5]. In this view, new alloys with improved tailored properties should be developed to further advance the PIM applications as well as to help to attain prices competitive to "conventional" ones.

Concluding remarks. The automotive sector has become a major consumer of PIM parts in Europe. Metallic parts of high complexity are used in ignition locks, as gearbox components, in the steering, in engines, in sensors, car seats, turbochargers, convertible bonnet driving and locking mechanisms, etc.[27] In Japan major automotive applications consist in steering systems components being produced in quantity of 400 000 parts/month[28] (PIM technique is usually competitive to metallurgic processes starting with production of 50 000 parts/year). PIM components for applications at the extreme low temperatures with the potential use in the hydrogen storage tank of the BMW Hydrogen 7 are currently developed in Austria[29].

At present demands on multiphase PIM materials are stringent. It is obvious that reliable simulations of the PIM process can only be performed when the material parameters are known with sufficient accuracy. Processing of PIM materials is clearly an interdisciplinary challenge, combining metallurgy with plastic processing and material science of polymer resins. However, the design methodology currently developed in the PIM industry is based on the trial and error approach. The present state might be partly affected by the fact that majority of PIM realizations is patented, and the research groups involved do not will to publish their findings.

This work has been financially supported by the Grant Agency of the Czech Republic (project 103/08/1307) and Ministry of Education, Youth and Sports of the Czech Republic (project no. MSM 7088352101). B.H. is the laureate of the national section "For Women in Science", being financially supported by L´Oréal during the year 2007.

REFERENCES

1. German R. M., Bose A., in: *Injection Molding of Metals and Ceramics*. MPIF, Princeton 1997.
2. Hausnerová B., Sáha P., Kubát J.: Int. Polym. Proc. *14*, 254 (1999).
3. Hausnerová B., Sáha P., Kubát J., Kitano T., Becker J.: J. Polym. Eng. *20*, 237 (2000).
4. Dihoru L. V., Smith L. N., German R. M.: Powder Metall. *43*, 31 (2000).
5. German R. M., in: *Powder Injection Moulding*. MPIF, Princeton 1995.
6. Nielsen L. E., in: *Polymer Rheology*. Marcel Decker, New York 1977.
7. Chong J. S., Christiansen E. B., Baer A. D.: J. Appl. Polym. Sci. *15*, 2007 (1971).
8. Maron S. H., Pierce P. E.: J. Colloid Sci. *11*, 80 (1956).
9. Jorge H. R., Correia A. M., Cunha A. M.: ANTEC *2005*, 605.
10. Honek T., Hausnerová B., Sáha P.: Polym. Comp. *26*, 29 (2005).
11. Barreiros F. M., Vieira M. T.: Ceram. Int. *32*, 297 (2006).
12. Hausnerova B., Sedlacek T., Slezak R., Saha P.: Rheol. Acta *45*, 290 (2006).
13. Schlieper G.: Powder Injection Mould. Int. *2*, 21 (2008).
14. Urval L., Lee S., Atre S. V., Park S.-J., German R. M.: Powder Metall. *51*, 133 (2008).
15. Hsu K. C., Lo G. M.: Powder Metall. *39*, 286 (1996).
16. Murray J. S. Jr., in: *X-Stat Statistical Experiment Design/ Data Analysis/Nonlinear Optimization*. John Wiley, New York 1984.
17. Kurzbeck S., Kaschta J., Münstedt H.: Rheol. Acta *35*, 446 (1996).
18. Hausnerová B., Honek T., Sáha P., Kitano T.: J. Polym. Mat. *21*, 1 (2004).
19. Husband D. M., Aksel N.: J. Rheol. *37*, 215 (1993).
20. Hoffman R. L.: Trans. Soc. Rheol. *16*, 155 (1972).
21. Barnes H. A.: J. Non-Newtonian Fluid Mech. *56*, 221 (1995).
22. Honek T., Hausnerová B., Sáha P.: Appl. Rheol. *12*, 72 (2002).
23. Hatzikiriakos G. S., Dealy J. M.: J. Rheol. *36*, 703 (1992).
24. Chuankrerkkul N., Messer P. F., Davies H. A.: Powder Metall. *51*, 72 (2008).
25. German R. M.: Powder Injection Mould. Int. *2*, 18 (2008).
26. Dowson G., Williams B., in: *Metal Injection Moulding*. EPMA, Shrewsbury 1995.
27. http://www.piminternational.com/aboutpim/application
28. Williams N.: Powder Injection Mould. Int. *2*, 37 (2008).
29. Williams N.: Powder Injection Mould. Int. *1*, 5 (2007).

KL-05
PLASTICIZATION IN COMPLEX, PHASE-SEPARATED POLYMERS

E. BRUCE ORLER[a], REX. P. HJELM[b]*, JOSEPH T. MANG[c], DEBRA A. WROBLESKI[a], DAVID A. LANGLOIS[a], and MARILYN E. HAWLEY[a]

[a] Materials Science and Technology Division, Los Alamos National Laboratory; [b] Los Alamos Neutron Science Center, Los Alamos National Laboratory, H-805, Los Alamos New Mexico 87455, USA, [c] Dynamic Experimentation Division, Los Alamos National Laboratory*
hjelm@lanl.gov

Plasticizers reduce the bulk modulus and T_m of polymer materials; thus, they are of commercial importance as processing aids. A nitroplasticizer (NP) is used to soften a polyurethane binder, Estane, to lower the temperature at which Estane bound composites can be molded. The effect of NP on Estane mechanical properties is significant. Young's modulus, for example, for Estane is 5 MPa (ref.[1]), whereas the value for plasticized Estane is 0.7 MPa (ref.[2]). We aim to determine the poorly understood nanoscale mechanisms that lead to the softening of a thermoplastic, such as Estane.

Segmented polyurethanes, such as Estane, consist of crystalline aromatic, hard segments, randomly covalently linked with soft, rubbery segments. Previously we showed in, Estane, which has a low, 23 % by weight, hard segment content, that the hard segments partially phase segre-gate into small, discrete domains embedded in a matrix rich in rubbery segments. We postulated that the discrete domains act as reinforcing fillers[3].

We used small-angle neutron scattering (SANS) data and the difference in scattering between NP mixtures containing different fractions of NP and deuterated NP (d-NP), f_D, to determine the distribution of NP in Estane and its effect on the nano-scale structure. The method was the same used to extract the composition and structure of neat Estane by swelling with mixtures of protonated and deuterated solvents[3].

SANS data was analyzed assuming that the discrete domain structure is described by a micelle model[3], in which the dis-crete domains have a uniform core, surrounded by a corona of tethered polymer intermixed with the matrix. Whereas the core consists mainly of hard segment, it contains a significant component of soft seg-ment. Conversely, the matrix consists mostly of soft segment, but also contains a significant amount of hard seg-ment. The corona is chemically identical to the matrix, but is distnquished by taking up less solvent when Estane is swollen with different solvents.[3]

With increasing content of NP from 10 to 50 % by weight the T_g associated with soft segments decreased from ca −35 C to −50 C. The endotherm associated with T_m of the discrete do-mains decreased slightly from ca 60 C and its integrated area decreased by roughly a factor of 2. Young's modulus decreased by an amount that was far greater than predicted by dilution effects of the matrix. When d-NP is used, a peak in the Estane SANS data was seen to decrease in intensity with the amount of d-NP present up to about 20 % by weight, then increase. These results indicated that the NP interacts with the matrix and has an effect on the discrete domains.

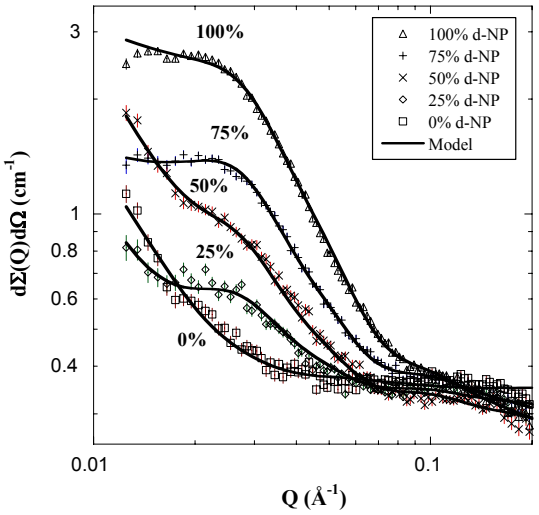

Fig. 1. **Contrast-dependent SANS**

In Estane formulated with 50 wt.% NP a SANS peak appears and its intensity becomes larger with increasing f_D (Fig. 1). The peak is positioned at lower Q than in Estane[3], consistent with a greater concentration of NP in the matrix and increased spacing between the domains in plasticized Estane.

Analysis of the data by the micelle model, (Fig. 1), showed that the bulk of the NP was taken up by the matrix and that there was a significant plasticizer in the core. However, there was no change in either the core radius, 2.95±0.01 nm or in soft segment content, 0.37±0.01, in plasticized Estane compared to Estane[3]. There was less hard segment content in the core, 0.34±0.01, relative to neat Estane, 0.7±0.1 (ref.[3]). The corona included less NP than the matrix, suggesting that the core in plasticized Estane affects the micromechanics of the surrounding volume in the same way as observed in Estane[3].

We gain insight on the effect of NP in Estane by comparing the discrete domain density corrected for the volume change due to NP, $5.1 \pm 0.3 \cdot 10^{16}$ cm^{-3}, with that for neat Estane, $1.0 \pm 0.1 \cdot 10^{17}$ cm^{-3} (ref.[3]). Thus, the effect of NP on Estane is consistent with the hypothesis that the mechanism of softening by NP is by inhibiting the forma-tion of the filler-like discrete domains.

This work benefited from the use of LQD at the Manuel Lujan, Jr. Neutron Scattering Center of the Los Alamos National Laboratory and was supported by the US. Department of Energy.

REFERENCES

1. Banergee B., Cady C. M., Adams D. O.: Modeling Simul. Mater. Sci. Eng. *11*, 457 (2003).
2. Cady C. M., Blumenthal W. R., Gray G. T. III, Idar D. J.: Polym. Sci. Eng. *46*, 812 (2006).
3. Mang J. T., Hjelm R. P., Orler E. B., Wrobleski D. A.: Macromolecules *41*, 4358 (2008).

KL-06

POLYCAPROLACTONE – WOOD PARTICLES BIODEGRADABLE COMPOSITES MODIFIED BY THERMAL DECOMPOSITION OF ORGANIC PEROXIDE

IVAN CHODÁK*, ZUZANA NÓGELLOVÁ, and IVICA JANIGOVÁ

Polymer Institute, Slovak Academy of Sciences, Dúbravská cesta 9, 842 36 Bratislava, Slovakia
upolchiv@savba.sk

Biodegradable plastics attract an increased interest as environmentally friendly materials. The high volume applications can be also considered for automotive especially for interior parts. Besides natural look and light weight, simple waste management is also important in this case since recycling of cars is of rising consent recently. However, a broad application is partially hindered by unsuitable properties and by the high price of biodegradable plastics, compared to conventional materials, especially polyolefins. Rather inexpensive way consists in a preparation of two – phase materials via either blending with another polymer or preparation of composites by addition of a filler[1]. Both routes usually require certain level of adjustment of interactions on the phase boundaries by an addition of compatibilizers as a separate component of the mixture[2] or by chemical modification of either matrix or filler surface[3]. Certainly, when dealing with environmentally degradable plastics, any modification can be only considered if the resulting material is also environmentally degradable. From this point of view, the mixing with various types of cellulose – based particles is an obvious option. In this case, besides modification of certain properties, a decrease of the price of the material can be expected as well.

In this paper, biodegradable matrix filled with organic filler has been discussed. Polycaprolactone (PCL) was used as the biodegradable matrix. The disadvantages connected with this polymer can be summarized as low melting temperature resulting in a low deflection temperature, relatively low tensile strength and modulus, and rather high price compared to high volume common plastics, e.g. polyolefins. On the other hand, high toughness and elongation at break, biodegradability and resistance towards thermal degradation as well as good processability can be mentioned as advantages of PCL.

If organic fillers such as sawdust or switchgrass are used as a composite component, usually a compatibilizer has to be used to improve the interaction between hydrophobic polymer matrix and hydrophilic surface of the filler. Various compatibilizers have been used, the most common being the parent matrix polymer functionalized by maleic anhydride[4]. In the past we investigated the crosslinking initiated by thermal decomposition of an organic peroxide to achieve a compatibilizing effect in a composite based on low density polyethylene as a model matrix and various organic fillers such as birch wood particles[5], aspen fibers, recycled paper, rubber crumb etc.[6]. A formation of covalent bonds leading to grafting of the polyethylene chains onto filler surface was proposed based on SEM observation[7]; this model is in accordance with mechanical properties, especially with an unexpected large increase in Young's modulus for crosslinked composites in spite of a decrease in the crystallinity of the matrix due to crosslinking[8].

The effect similar to crosslinking regarding mechanical properties was observed also if 10 to 30 wt.% of functionalized polyethylene was added to LDPE / wood flour composite. In this case a copolymer polyethylene – co – acrylic acid was found as an efficient modifier[9].

In this paper, a formation and properties of biodegradable composites with polycaprolactone matrix were investigated. A mixture of polycaprolactone (CAPA 6800, Solvay) with switchgrass (supplied by Univ. Québec Trois-Rivières) was chosen as an example of biodegradable filler in biodegradable matrix. 2,5-dimethyl-2,5-ditertbutyl peroxyhexyne (Luperox 130, Luperco, Germany) was used as the initiator of crosslinking.

The composites were prepared by melt mixing all components in a Plasti-Corder kneading machine PLE 330 (Brabender, Germany) at 120 °C for 10 minutes. Test specimens were prepared by compression molding at 120 °C for 2 minutes and at 180 °C for 20 minutes for uncrosslinked and crosslinked materials, respectively. The peroxide has been completely decomposed under given conditions. The dog – bone specimens for testing the mechanical properties were cut at room temperature using a specially shaped knife. Mechanical properties were measured using the Universal testing machine INSTRON 4301 at RT at deformation rate 10 mm / minute. Thermal parameters of samples were measured using DSC 821^e (Mettler-Toledo) in nitrogen atmosphere. Heat of fusion and melting temperature was determined from the second heating scan. Brittle fracture surfaces of notched samples for SEM observation were prepared at a liquid nitrogen temperature. Scanning electron microscope JSM 6400 (JEOL, Japan) was used for micrographing.

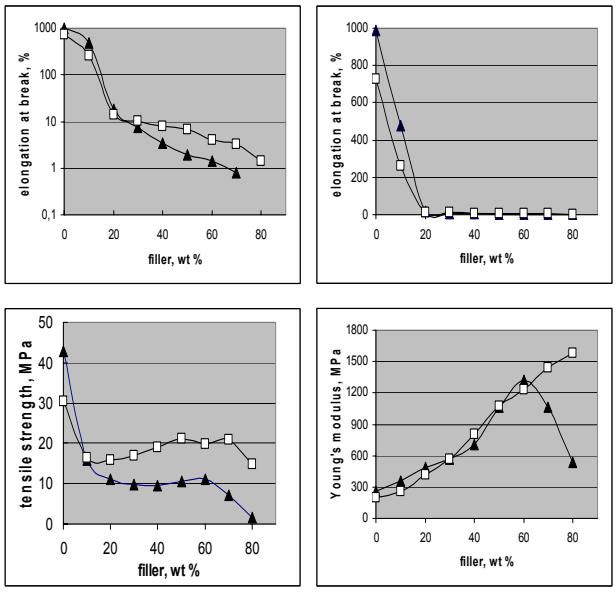

Fig.1. **The dependences of mechanical properties on the filler content for uncrosslinked (full triangles) and crosslinked (open squares) polycaproplactone filled with switchgrass**

The effect of the filler content for uncrosslinked and crosslinked mixtures is seen in Fig. 1. The effect of both the filler content increase and the crosslinking is similar to the one observed for polyethylene filled with organic fillers[5,6]. The increase in the filler content leads to an increase in Young's modulus and a decrease in the elongation at break. This behaviour is generally common for most of two-phase polymeric systems if a stiff component is mixed into a ductile matrix.

Crosslinking results in certain changes in the dependences of mechanical properties on the filler content. First, it is seen that crosslinking leads to a decrease in Young's modulus, tensile strength and elongation at break for PCL without filler. The decrease in modulus can be ascribed mainly to the drop in the crystallinity degree in the virgin polymer (see Fig. 3). As seen in Fig. 1, the same effect regarding both mechanical properties and melting parameters was observed also for composites with low amount of the filler. With rising filler content, the effect of crosslinking on mechanical properties is changing. In spite of decreased crystallinity, modulus of crosslinked PCL / switchgrass composite with the filler content above 30 wt.% is higher compared to the uncrosslinked composites with the same concentration of the filler.

This behaviour is similar to that observed for LDPE / organic filler composites and has been ascribed to a formation of covalent bonds between polymeric chains and the filler surface. Grafting of the polymer occurs on the filler surface, leading to an increased adhesion on the phase boundaries. Consequently, more compact material is formed with fewer voids formed during the sample preparation, containing smaller number of weak units where crack could be easily formed. This is clearly seen especially at filler content above 60 wt.% where uncrosslinked composites suffer from many defects, resulting in a decrease of modulus (presumably due to a formation of number of voids leading to a decrease in effective cross section of the specimen) while a permanent increase in the modulus values for crosslinked samples is observed, up to impressive 1.5 GPa. Obviously, improved adhesion of the part of polymeric matrix onto filler surface results in a formation of much more compact materials with lower number of defects.

The increased adhesion of the matrix polymer onto filler surface due to crosslinking was directly observed by SEM, as seen in Fig. 2, where fracture surfaces of composites containing 50 wt.% of the filler are shown. The filler surface of uncrosslinked material is almost clean from the polycaprolactone, while for crosslinked composite remnants of the polymer attached to the surface is clearly observed.

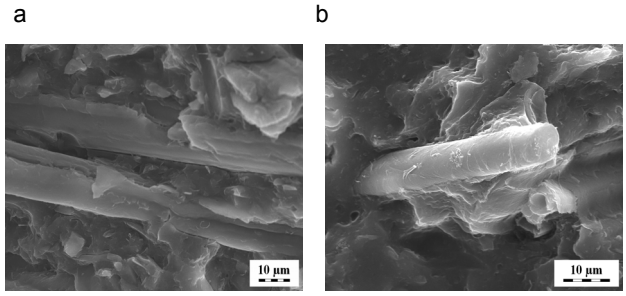

Fig. 2.

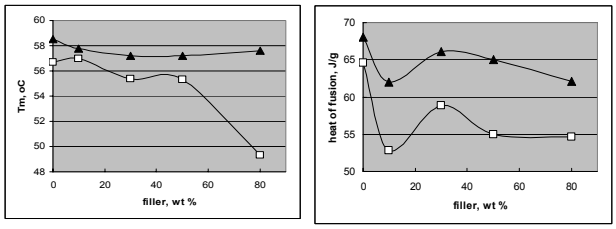

Fig. 3. **Melting temperature and heat of fusion of uncrosslinked (full triangles) and crosslinked (open squares) polycaprolactone composites in dependence on the switchgrass filler content**

On the other hand, a decrease in elongation at break as a result of crosslinking can be ascribed to a decrease in the chain mobility due to cross bonds introduced. These tendencies are observed for the unfilled PCL and composites with low amount of the filler, up to about 20 wt.%. With rising filler content, the behaviour is changing. In this case, crosslinking results in an increase in deformability partially due to lower crystallinity but mainly resulting from higher resistance to crack formation on the polymer – filler phase boundaries as discussed in[10].

Tensile strength curves shown in Fig. 1 indicate that this parameter depends on both modulus and deformation values. Growing modulus contributes to an increased strength but the same is true for elongation at break, namely due to possible elongation strengthening at high deformation, but generally simply because at similar modulus more energy is required to break the sample if deformation is higher. A decreased number of defects on the polymer – filler boundaries contributes to an increased tensile strength as a result of crosslinking.

The melting parameters (melting temperature and heat of fusion proportional to overall crystallinity) are shown in Fig. 3 in dependence on the filler content for crosslinked and uncrosslinked samples. Crosslinking leads to lower melting temperature obviously due to the fact that crosslinking represents a defect in the polymeric chain, resulting in shorter folds forming crystals. It is understandable that lower amount of the polymer can crystallize if more defects are introduced in the chains leading to lower values of the heat of fusion.

Thus, it can be concluded that treating the polycaprolactone / switchgrass composites with organic peroxide results in an increase of polymer adhesion on the filler surface as indicated by mechanical properties, scanning electron microscopy and melting parameters. The observed changes in mechanical properties are interpreted as a uperposition of improved interactions on the phase boundaries and a decrease in crystallinity.

The research was supported by the Slovak Research and Development Agency APVV, grant No 51-010405.

REFERENCES

1. Biodegradable Polymers, Principles and Applications, (Scott G., ed). Kluwer Acad. Publ., Dordrecht 2002.
2. Zuchowska D., Steller R., Meissner W.: Polym. Degrad.

Stab. 60, 471 (1998).
3. Bikiaris D., Prinos J., Koutsopoulos K., Vourotzis N., Pavlidou E., Frangis N., Panayiotou C.: Polym. Degrad. Stab. 59, 287 (1998).
4. Maldas D., Kokta B. V.: J. Adhes. Sci. Technol. 8, 1 (1994).
5. Nógellová Z., Kokta B. V., Chodák I.: J. Macromol. Sci., A, Pure Appl. Chem. 35, 1069 (1998).
6. Chodák I., Nógellová Z., Kokta B. V.: Macromol. Symp. 129, 151 (1998).
7. Janigová I., Lednický F., Nógellová Z., Kokta B. V., Chodák I.: Macromol. Symp. 169, 149 (2001).
8. Chodák I.: Progr. Polym. Sci. 20, 1165 (1995).
9. Sedláčková M., Lacík I., Chodák I.: Macromol. Symp. 170, 157 (2001).
10. Chodák I., Chorváth I.: Macromol. Symp. 75, 167 (1993).

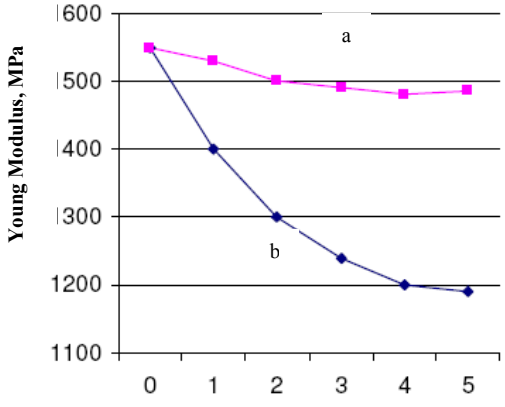

Fig. 1. **Young modulus of recycled polycarbonate:** a) dryed; b) wet

KL-07
RECYCLING OF PLASTIC COMPONENTS IN THE CAR LAMPS

MAREK KOZLOWSKI and STANISLAW FRACKOWIAK

Wroclaw University of Technology, Faculty of Environmental Engineering, Laboratory of Advanced Polymeric Materials and Recycling, Wybrzeze Wyspianskiego 27, 50-370 Wroclaw, Poland
marek.a.kozlowski@pwr.wroc.pl

Introduction

Plastics represent a steadily increasing share among the materials used for construction of automobiles. These materials are advantageous in comparison to metals because plastics do not rust, are easily processable, highly aesthetic, safe and comfortable in use. However, a main merit is that a density of plastics is a few time lower than that of steel or cast iron. With a vehicle mass saving one can reduce a fuel consumption, thus contributing to an improvement of environment by means of reducing CO_2 emissions and by savings the natural resources (crude oil). The material savings are related to recovery and recycling of plastic parts from the end of use vehicles. This possibility is directly related to the required quota of the materials re-use and recycling according to the ELV Directive 2000/53/CE (currently 85 wt.% and 95 wt.% till 2015). Among recovery methods the mechanical recycling (reprocessing) has a well established position for its simplicity and economy. However, the economical profits depend on a kind of the polymer to be recycled. As a rule, recycling of the commodity plastics is hardly profitable (besides large, easy to dismantling parts), because the costs of technology are higher than the difference in price between the virgin resin and recylate. Much more profits one can expect from the mechanical recycling of engineering plastics, which price of a virgin polymer is high. To this group of plastics belong polycarbonate (PC), polyamide (PA), ABS, POM, PMMA, PBT. Among the parts constructed with these polymers are the front and rear lamps. The headlamps are made of polycarbonate, whereas in the tail lights besides PC also ABS and PMMA is used. Recycling of these plastic has been discussed in this paper.

Teh easiest way of waste management is regrinding and reprocessing into a form of pellets. Unfortunatelly, during these processes a degradation of polymers takes place. This results in a deterioration of the mechanical properties of recyclates. The extent of degradation depends both on the equipment used for recycling (grinders, dryers, extruders), operating parameters and on a nature of the polymer. Some polymers are sensitive to moisture, whereas others can reprocessed several times without any visible influence on their properties.

Possible changes have been presented in Fig. 1 for polycarbonate. While recycled in dry conditions, PC retains high stiffness even after five recycling stages. If avoiding drying, the mechanical properties of polycarbonate drop dramatically after each recycling. Deterioration of properties can be reduced by blending of a recyclate with other polymers or fillers. Such possibilities have been attempted and the results have been presented in this paper.

Experimental

The polymers used for the study were: polycarbonate Makrolon (Bayer), polymethyl methacrylate PMMA 920 (Altuglas) and ABS copolymer. For compatibilization of blends a maleated copolymer Kraton SEBS-g-MA was used.

Polymer composites were manufactured by addition of following fillers: unmodified montmorillonite Nanomer PGW (Nanocor), organically modified montmorillonites Nanomer I30.P, Nanomer I44.P (Nanocor) nanometric calcium carbonate NPCC (NanoMaterials Technology).

Composites manufactured with PC, ABS, PMMA and respective fillers (5 wt.%) were prepared by melt mixing with a periodic mixer Haake (220–235 °C depending on a matrix polymer).

Melt rheology was measured with HAAKE Rotovisco RT20 rheometer. Mechanical properties were evaluated with a tensile machine Lloyd LR10k or an impact tester Resil 5.5 (Ceast).

Results

Rheological measurements have revealed that reprocessing does not influence markedly ABS and PMMA – the viscosity curves remain almost at the same level after four recycling stages (Fig. 2 and 3). This finding are contradictory to that received for recycling of polycarbonate, especially if the polymer was not dryed.

Application of silica and $CaCO_3$ as fillers have revealed that the properties of composites are related to a kind of the inter-gallery modifier in a montmorillonite filler. The shape of a filler (cubic versus platelet) also plays a role for a final characteristics of composites.

Polycarbonate has revealed as an extremely sensitive polymer to a degradation caused by the thermal and mechanical stresses.

More promising results have been received for the blends prepared from the polymers studied (Fig. 4). Combination of different viscoelastic characteristics od PC and ABS resulted in a high impact of blends, especially after compatibilization with a maleated copolymer SEBS-g-MA.

Conclusions

Waste plastics form the vehicle lightings may serve as a source of promissing materials for new blends of attractive properties.

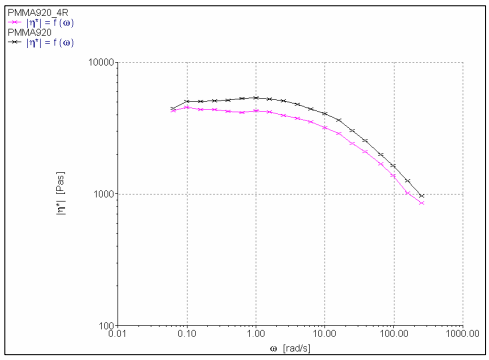

Fig. 2. **Melt viscosity of virgin PMMA and after 4 reprocessings**

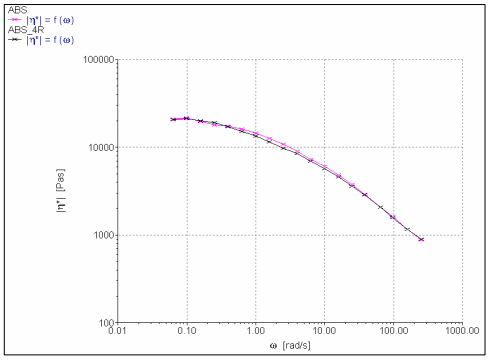

Fig. 3. **Melt viscosity of virgin ABS and after 4 recycling stages**

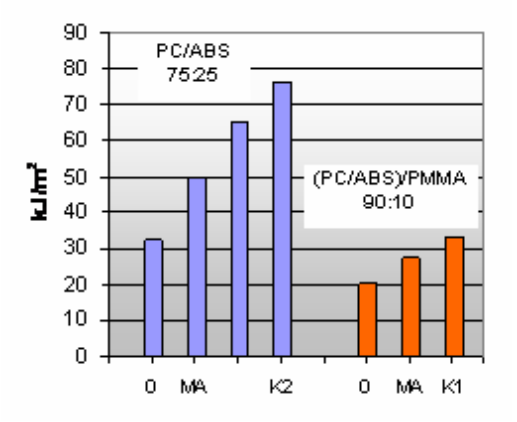

Fig. 4. **Charpy impact strength for PC/ABS blends and alloys**

Polymer composites based of engineering polymers filled with the fillers of nanometric size do not guarantee the mechanical properties of high interest to automotive industry. For a successful application of the composites made of waste polymers used for automotive lightings a thorough design and sophisticated materials science knowledge should be applied.

KL-08
VERY FAST VULCANISING SYSTEMS

ANTONÍN KUTA, ZDENĚK HRDLIČKA, and VRATISLAV DUCHÁČEK

Institute of Chemical Technology, Department of Polymers, Technická 5, 166 28 Praha 6, Czech Republic
antonin.kuta@vscht.cz

Abstract

Sulphur vulcanising systems with zinc isopropyl xanthate (ZIX) and zinc diethyl dithiocarbamate (ZDEC) have been used for dry natural and synthetic rubbers (NR and SR). Curing process of NR has been faster than that of SR. The biggest difference has been found for standard emulsion type of styrene-butadiene rubber (E-SBR). Retarding influence of acids originated from an emulsifier could play a role. A solution type of SBR (S-SBR) and other SR without acidity have been tested as well. Curing process was still slower than that of NR. Good results for E-SBR have been obtained when combinations of tetramethylthiuram disulfide (TMTD) with thiourea (TU) without elementary sulphur were used.

Xanthate and carbamate accelerators cure common types of NR reasonably faster than common highly unsaturated types of synthetic rubbers. Cure rate and cure efficiency of conventional and efficient vulcanising systems with ultra accelerators depend on “impurities” in raw NR.

Introduction

Very fast vulcanising sulphur systems due to their high activity are used for vulcanisation of highly unsaturated rubbers at low temperatures or low unsaturated rubbers at common (higher) temperatures.

Very fast rubber vulcanisation is usually achieved by vulcanising systems with ultra accelerators. Zinc salts of xanthates and dithiocarbamates are typical representatives of them. It has been also suggested that thiourea can be used as a secondary accelerator to the primary one, such TMTD to reach fast vulcanisation[1,2].

Ultra accelerators are typically used for vulcanisation of natural rubber in the latex form. Vulcanisation of latex products is usually carried out at lower temperatures compared to dry rubber products. Cure activity of ultra accelerators in highly unsaturated synthetic rubbers (SR) is expected also to be high, however, lower than in natural rubber (NR), e.g. in emulsion type of SBR (E-SBR).

Material and methods

Rubbers:
Natural Rubber (NR)*;* Malaya Rubbers, Malaysia
SMR 20, SMR 10, pale crepe
deprotenized NR (DPNR)
Isoprene rubber (IR)
SKI-3, Nizhnekamskneftechim Inc., Russia
Butadiene rubber (BR),
SKD, Efremov Synthetic Rubber Enterprise Join Stock Co., Russia
Buna cis 132 - Schkopau, Dow Plastics
Styrene-butadiene rubber, emulsion type (E-SBR)
Kralex 1500, Synthos Kralupy a.s., Czech Republic
Buna SB 1500 Schkopau, Dow Plastics
Styrene-butadiene rubber, solution type (S-SBR),
Calprene 1204B, Dynasol Elastomers, S.A., Spain
BUNA VSL 5025-0 HM, Lanxess, Germany
SE SLR-4601, Dow Plastics

Accelerators:
Zinc diethyl dithiocarbamate (ZDEC), *Robac ZDEC*; Robinson Brothers, UK
Zinc isopropyl xanthate (ZIX), *Robac ZIX*; Robinson Brothers, UK

Formulation of rubber compounds were as simple as possible, to allow clearly observe the rubber curing nature. "Conventional" (C) and "efficient" (EV) vulcanising systems were used. The formulations are shown in Table I.

The course of vulcanisation has been recorded by Rubber Process Analyzer 2000 (Alpha Technologies) at temperature range from 140 °C to 80 °C.

Rubber vulcanisation activity was evaluated as cure rate and cure efficiency.

The term cure rate R_v means an average cure rate, which has been calculated via the simplest method:

$$R_v = \frac{1}{t_{90} - t_{10}}$$

where t_{90} (t_{10}) is time required to reach 90 % (10 %) of maximum cure degree.

Table I
Formulation of rubber compounds

	ZIX-C	ZIX-EV	ZDEC-C	ZDEC-EV
Rubber	100	100	100	100
ZnO (phr)	5	5	5	5
Stearic acid (phr)	1	1	1	1
ZIX (phr)	1	4	–	–
ZDEC (phr)	–	–	1	4
Sulphur (phr)	2.5	1	2.5	1

Table II
Ash content and the relative absorption *I* of NR and SR at selected bands

Rubber	Ash [wt.%]	I_{1541}	I_{1633}
SMR 20	1.36	0.020	0.046
SMR 10	1.40	0.009	0.024
Crepe	1.25	0.004	0.021
DP NR	0.05	0.002	0.062
SKI-3	< 0.05	0	–

Cure efficiency has been expressed as a difference between maximum and minimum values of modulus (torque) $M_{max} - M_{min}$.

Impurities in NR have been quantified (Table II) as an ash content and by infrared spectroscopy as the relative absorption *I* (related to vibration C=C bond) at 1541 cm^{-1} band, if it was accompanied with the absorption band at 1633 cm^{-1} as a measure of protein content.

Results and discussion

Very low activity of xanthate ultra-accelerators in common SBR was the main reason for this study. Faster sulphur vulcanisation of NR compare to E-SBR is well known. However, the cure rate differences have been much larger when mercaptobenzothiazole (MBT) or sulphenamide accelerators are used. For example, cure rate at 140 °C of NR with MBT is 0.14 min^{-1} and E-SBR 0.018 min^{-1}, NR/SBR cure rate ratio is 7.8. For the ultra-accelerator studied (ZIX) this ratio was around 100. Cure rate values at 140 °C are summarized in Table III.

Main reason for cure rate differences is the presence of "impurities" or some additives in rubber. Acids are typical vulcanisation retarders, basic substances on the contrary accelerate vulcanisation. Organic acids in E-SBR originated from emulsifier are an example of the first group. Nitrogen containing bases (trigoneline, stachydine, choline, trimethyl amine)[3] which are present in fresh NR latex or are generated from proteins during latex processing and rubber storage are the examples of the second group.

Acidity of E-SBR has been our first explanation of dif-

Table III
Average cure rate R_v (min^{-1}) of NR and SR at 140 °C

Rubber	ZIX-C	ZIX-EV	ZDEC-C	ZDEC-EV
NR (*SMR 20*)	1.36	0.93	0.52	1.08
NR (*SMR 10*)	1.40	0.76	0.55	0.95
NR (*crepe*)	1.25	0.89	0.42	0.51
DP NR	0.83	0.52	0.48	0.35
IR (*SKI-3*)	0.86	0.56	0.52	0.38
E-SBR (*Kralex 1500*)	0.010	0.013	0.101	0.041
E-SBR (*Buna SB 1500*)	0.011	0.034	0.101	0.096
S-SBR (*Calprene*)	0.35	0.32	0.121	0.126
S-SBR (*Buna VSL*)	0.181	0.31	0.116	0.133
S-SBR (*SLR-4601*)	0.57	0.36	0.25	0.198
BR (*SKD*)	0.72	0.72	0.20	0.149
BR (*Buna cis*)	0.47	0.35	0.169	0.157

Table IV
Maximum cure degree M_{max}–M_{min} (dNm) of NR and SR at 140 °C

Rubber	ZIX-C	ZIX-EV	ZDEC-C	ZDEC-EV
NR (*SMR 20*)	10.7	10.9	14.3	9.7
NR (*SMR 10*)	10.4	8.4	14.0	9.2
NR (*crepe*)	3.3	7.4	12.7	9.1
DP NR	4.6	5.0	10.4	6.9
IR (*SKI-3*)	3.4	9.3	9.4	5.7
E-SBR (*Kralex 1500*)	5.6	0.7	20.9	10.6
E-SBR (*Buna SB1500*)	2.8	0.5	19.6	8.6
S-SBR (*Calprene*)	10.9	14.2	22.2	9.0
S-SBR (*Buna VSL*)	2.5	1.1	18.4	7.0
S-SBR (*SLR-4601*)	3.5	2.9	17.0	7.5
BR (*SKD*)	13.8	17.5	20.3	14.4
BR (*Buna cis*)	5.1	5.6	18.4	8.6

ferences in curing activity of NR and E-SBR. To prove it, 2 phr of sodium carbonate or triethanol amine were added to a Kralex based compound to neutralise acids. The cure rate with ZDEC-C system at 140 °C increased from 0.1 min^{-1} to 0.12 min^{-1} and 0.21 min^{-1}, respectively.

The preparation of rubber compounds based on a solution type of SBR is another way how to obtain SBR compounds without acid emulsifier residues. The S-SBR compounds cured faster than E-SBR ones, especially with ZIX accelerator. However, the cure rate has been still lower then in NR.

S-SBR is not a simple copy of E-SBR without acids. Styrene units are also randomly distributed in macromolecular chains and their amount is similar (25 % in S-SBR and 23.5 % in E-SBR), but due to different polymerisation chemistry, butadiene units are more frequently bonded in 1,2 positions in polymer chains. Content of vinyl groups arising via this 1,2 addition is higher in S-SBR than in E-SBR, in our case 30 % compare to 18 %. That difference can also influence vulcanisation reactions.

To eliminate vinyl group effects and diluting effect of the inert comonomer, next rubber compounds have been prepared from high *cis*-1,4-polybutadiene. Although the cure rate of BR compound has been higher than S-SBR, the level of NR has not reached.

Cure rate of isoprene rubber (IR) as real synthetic analogue of NR has been the closest to NR. However, there are cure rate differences between NR grades. Cure rate of NR grades has increased in order DPNR < crepe < SMR 10 < SMR 20, i,e, with impurities content. Polyisoprenes with very low content of impurities (DP NR and SKI-3) have showed almost the same cure rates.

Conventional system with ZIX accelerator was always faster than EV system. On the other hand, the same system with carbamate accelerator was slower, except SKI and crepe at low temperatures.

Cure rate generally decreased with temperature decreasing. The effect of "impurities" and molecular structure at temperature range 140 °C to 80 °C was very similar – cure rate of NR increased with N content, E-SBR has been the slowest. It cured so slowly, that carbamate system has not been able to vulcanise below 120 °C, xanthate even below 140 °C. Good results have been obtained with another vulcanising system based on the combination of tetramethylthiuram disulfide (TMTD) with thiourea (TU) without elementary sulfur. Optimum dosage is 4 phr TMTD and 5 phr TU. Cure rate at 120 °C was 0.44 min^{-1}, at 100 °C 0.09 min^{-1} and at 90 °C still 0.03 min^{-1}. Curing time (t_{95}) of carbon black filled SBR compounds vulcanized at 100 °C lies in the range from 50 to 60 min (ref.[4]).

Maximal cure degree of rubbers has been also influenced by "impurities" content. The lowest cure degree of NR was reached in case of DP NR. Conventional carbamate system was the most efficient system in polyisoprenes. Cure degree reached with EV systems was mostly lower. Higher curative dosage could decrease system sensitivity on impurities. But very low cure degree and cure rate of ZIX-EV system in E-SBR is probably a result of accelerator decomposition by acidity due to low chemical stability of xanthates. M_{max}–M_{min} data at 140 °C as the maximal cure degree are summarized in Table IV.

Conclusions

Vulcanising activity of xanthate systems in emulsion type of SBR is very low, probably due to accelerator decomposition. Good result has been obtained with system based on the combination of tetramethylthiuram disulfide with thiourea.

Xanthate and carbamate accelerators based vulcanising systems cure NR reasonably faster than common highly unsaturated types of synthetic rubbers. There are cure rate differences between NR grades, cure rate increases with non-rubber substances content, namely with proteins.

The support of the Ministry of Education, Youth, and Sports of the Czech Republic (through research grant MSM 6046137302) is gratefully acknowledged.

REFERENCES

1. Ducháček V.: J. Appl. Polym. Sci. *22*, 227 (1978).
2. Mathew G., Kuriakose A. P.: J. Appl. Polym. Sci. *49*, 2009 (1993).
3. Suchiva K., Kowitteerawut T., Srichantamit L.: J. Appl. Pol. Sci. *78*, 1495 (2000).
4. Kuta A., Hrdlička Z., Ducháček V.: In: *IRC 2007*, Paper No. 161. Cleveland, OH, USA (2007).

KL-09
X-RAY NANO CT: 3D ANALYSIS OF COMPOSITE AND RUBBER MATERIALS WITH SUBMICROMETER RESOLUTION

JENS LUEBBEHUESEN and OLIVER BRUNKE

GE Sensing & Inspection Technologies GmbH (phoenix|x-ray), Niels-Bohr-Str. 7, 31515 Wunstorf, Germany
Jens.Lubbehusen@ge.com, www.phoenix-xray.com

During the last decade, Computed Tomography (CT) has progressed to higher resolution and faster reconstruction of the 3D-volume. Most recently it even allows a three-dimensional look into the inside of materials with submicron resolution. High-resolution X-ray CT allows the 3D visualization and failure analysis of the internal microstructure of composite materials – even where 2D X-ray microscopy would give only the integral information of the overlaying bundles of fibers. By means of nanofocus® tube technology, nanoCT®-systems are pushing forward into application fields that were exclusive to expensive synchrotron techniques. But their potential, convenience and economy of these lab systems is often underestimated.

Especially for modern composite and rubber materials which are used in very expensive or safety relevant applications, CT is ideal to accompany the product from development to final quality control. The tube based CT measurements for the study were performed with a granite-based phoenix|x-ray nanotom®-CT system (GE Sensing & Inspection Technologies GmbH, Wunstorf, Germany) equipped with a 180 kV / 15 W high-power nanofocus® tube with Tungsten or Molybdenum-Targets. The tube offers a wide range of applications from scanning low absorbing samples in nanofocus® mode with voxel resolutions <500 nm and high absorbing objects in high power mode with focal spot and voxel sizes of a few microns. The nanotom® is the first 180 kV nanofocus computed tomography system which is tailored specifically to high resolution applications in the field of material science and micro electronics. Therefore it is particularly suitable for nanoCT-examinations e.g. of polymeric and composite materials, metals and metal foams, ceramics etc.

The CT volume data set can be displayed in various ways; it can be sectioned and sliced in all directions, rotated and viewed from any desired angle. Highly applicable to a variety of fields, nanoCT can be a viable substitute for destructive mechanical slicing and cutting. Any internal difference in material, density or porosity within a sample can be visualized and data such as distances can be measured. Some of the many applications of nanoCT include the analysis of fiber textures, air inclusions or cracks in composite materials with voxel resolutions down to less than one micrometer.

The presentation will outline the hard- and software requirements for high resolution tube based CT and compare CT results of sophisticated conventional tube-based with synchrotron radiation based scans. It will showcase several quality control applications of different composite and rubber materials that were inspected with high resolution nanofocus® and microfocus CT.

KL-10
MODIFICATION OF POLYAMIDES PROPERTIES BY IRRADIATION

MIROSLAV MANAS, MICHAL STANEK, DAVID MANAS, MICHAL DANEK, and ZDENEK HOLIK

Tomas Bata University in Zlin, Faculty of Technology, Department of Production Engineering, TGM 275, 762 72 Zlin, Czech Republic
manas@ft.tub.cz

Abstract

Radiation processing involves the use of natural or man-made sources of high energy radiation on an industrial scale. The principle of the radiation processing is the ability of the high energy radiation to produce reactive cations, anions, and free radicals in materials. The industrial application of the radiation processing of plastic and composites includes polymerization, cross-linking, degradation and grafting. Radiation processing involves mainly the use of either electron beams from electron accelerators or gamma radiation from Cobalt-60 sources.

Radiation processing does not make the product radioactive. The majority of industrial applications of radiation processing are a cross-linking of wire and cable insulations, tube, heat shrink cables, components of tires, composites, moulded products for automotive and electrical industry etc. Another significant application of radiation processing is the sterilization of medical disposables. A comparison of the mechanical properties of natural and irradiated polyamide PA6 and PA6.6 (unfilled and filled – 30 % GF) is presented in this article.

Introduction

The cross-linking of rubbers and thermoplastic polymers is a well-proven process of the improvement of the mechanical and thermal properties. The chemical cross-

linking or rubber vulcanization is normally induced by the effect of heating after processing with the presence of a curing agent. The cross-linking process for thermosets is very similar. In thermosets the polymer molecules are also chemically linked due to heat after processing.

The irradiation cross-linking of thermoplastic materials via electron beam or cobalt 60 (gamma rays) is proceeding separately after the processing. The cross-linking level can be adjusted by the irradiation dosage and often by means of a cross-linking booster.

The main deference between beta and gamma rays lies in their different abilities of penetrating the irradiated material. Gamma rays have a high penetration capacity. The penetration capacity of electron rays depends on the energy of the accelerated electrons.

Due to electron accelerators, the required dose can be applied within seconds, whereas several hours are required in the gamma radiation plant.

The ability of penetrating the irradiated material are given in the Fig. 1.

The palleted products are conveyed trough the radiation field. The radiation dose is applied gradually, that is to say, in several stages, whereby the palleted products are conveyed around the radiation sources several times. This process also permits the application of different radiation doses from one product type to another. It can be used for irradiation of polyolefines, polyesters, halogen polymer and polyamids from thermoplastics group, elastomers and thermoplastic elastomers. Some of them need the addition of crosslinking agent.

The dimensional stability, strength, chemical resistance and wear of polymers can be improved by irradiation[2]. Irradiation cross-linking normally creates higher strength as well as reduced creep under load if the application temperature is above the glass transition temperature (T_g) and below the former melting point. Irradiation cross-linking leads to a huge improvement in resistance to most of the chemicals

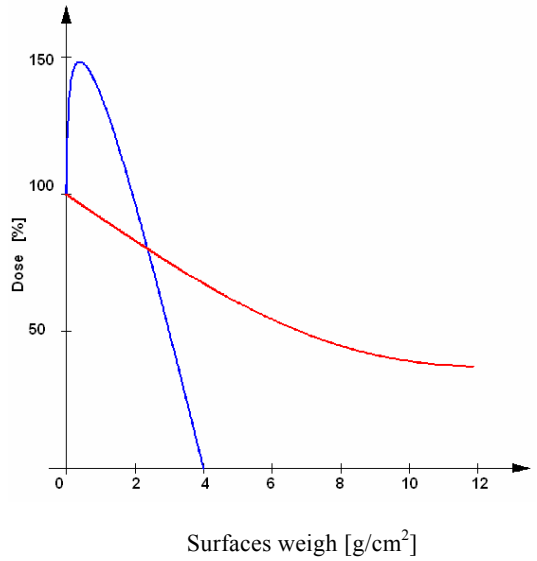

Fig. 1. **Ability of penetrating of electron – β and gamma – γ radiation**

and it often leads to the improvement of the wear behaviour.

The thermoplastics which are used for production of various types of products have very different properties. The main group presents standard polymers which are easy obtainable with favourable price conditions[3]. Limited level of both mechanical and thermal properties is big disadvantage of standard polymers. The group of standard polymers is the most considerable one and its share in the production of all polymers is as high as 90 %.

The engineering polymers are a very important group of polymers which offers much better properties in comparison to standard polymers. Both mechanical and thermal properties are much better than in case of standard polymers. The production of these types of polymers takes less than 10 %.

High performance polymers have the best mechanical and thermal properties but the share in production and use of all polymers is less than 1 %.

Still, it is necessary to say that in the decision-making process (which kind of polymers will be used) the application area and price are important. The differences in price are exorbitant – from unit euros (standard polymers) to tens or hundred euros per kg in case of some types of high performance polymers.

In connection with these data we have to ask if it is necessary to use engineering polymers or even high performance polymers in some application. In many cases it would be possible to use standard or engineering polymers and improve their properties, e.g. by irradiation.

The main objective of this study is investigation of influence of dose of irradiation on mechanical properties of polyamides PA6 and PA6.6 both without reinforcement and reinforced by 30 % of glass fibres.

Experimental

The properties not irradiated PA6 and PA6.6, both unfilled and filled 30 % glass fibres have been compared. The injection molding machine Arburg Allrounder 420C Advanced has been used for sample preparation.

Irradiation was carried out in the company BGS Beta Gamma Service GmbH & Co, KG, Saal am Donau, Germany with the electron rays, electron energy 10MeV, doses minimum of 66, 99, 132, 165 and 198 kGy.

Used polymers:
PA 6 – Frianyl B63 (unfilled)
PA 6 – Frianyl B63 GV30 (filled by 30 % glass fibers)
PA 6.6 – Frianyl A63 (unfilled)
PA 6.6 – Frianyl A63 GV30 (filled by 30 % glass fibers)

The tensile test with the use of stated equipment has been carried out:

Tensile test, according to standard CSN EN ISO 527 – 1, 527 – 2.
Equipment: Tensile test machine ZWICK 1456
SW – Test Xpert Standard
Temperatures: 23, 80 °C

To be able to state the effect of irradiation on net creation in the polymer structure the cross – linking grade has been determined (measured by Xylos gel test) for each type of

tested polyamide and the doses of irradiation. The results of gel test are given in the Fig. 2.

The irradiation radically improves the crosslinking grade of both filled and unfilled polyamides. The cross – linking grade of filled polyamides is about 15 to 20 % higher in comparison with the unfilled polyamides. The cross – linking improves the tensile strength and E modulus. The results on tensile strength of unfilled polyamides PA6 and PA6.6 are given in Fig. 3 and 4.

The results show the improvement of the ultimate tensile strength after irradiation by the dose of 66 kGy and its further slow increasing with the higher dose of irradiation.

The improvement of tensile properties is remarcable also in case of PA6 and PA6.6 both filled by 30 % glass fibres (Fig. 5 and Fig. 6). All test were carried out the temperature 23 °C.

The results of tensile tests at the temperature 80 °C are given in the Fig. 7 and Fig. 8. There are visible differences of ultimate tensile strength between irradiated and not irradiated tested polyamides.

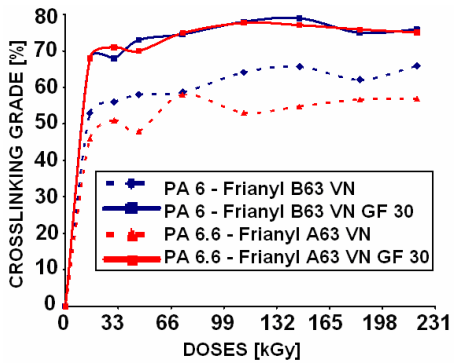

Fig. 2. **Comparison of Gross – linking grade of tested polymers**

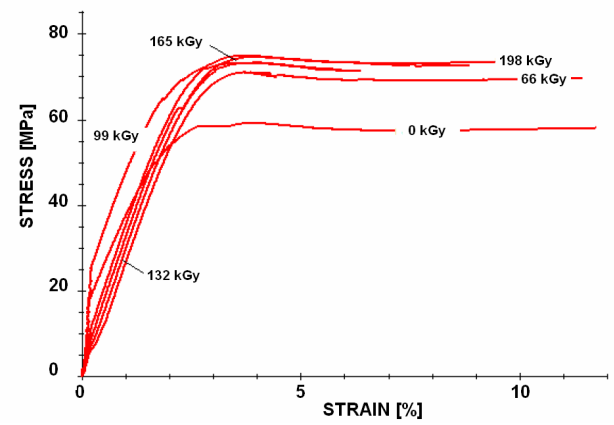

Fig. 3. **Tensile test** (PA6 at 23 °C)

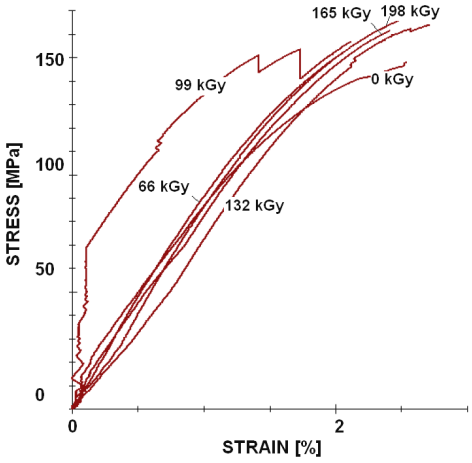

Fig. 4. **Tensile test** (PA6, 30 % GF at 23 °C)

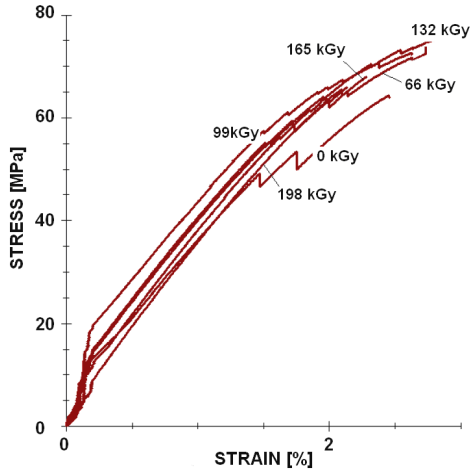

Fig. 5. **Tensile test** (PA6.6 at 23 °C)

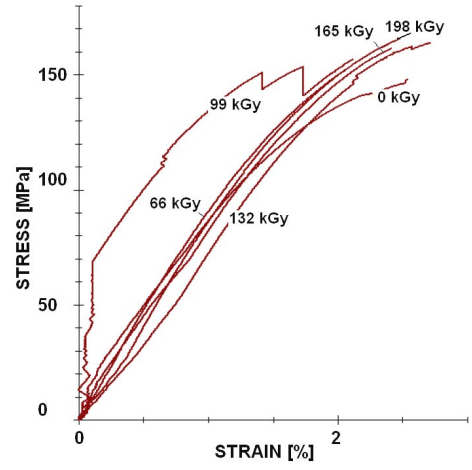

Fig. 6. **Tensile test** (PA6.6, 30 % GF at 23 °C)

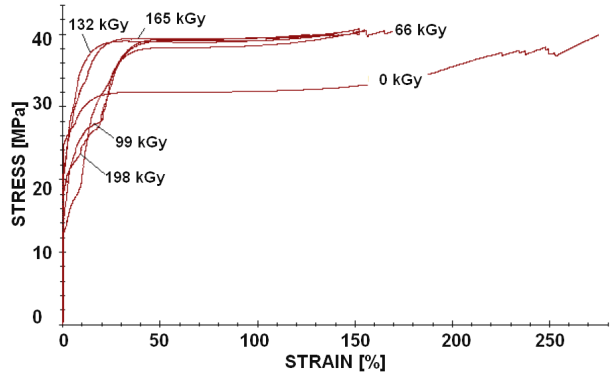

Fig. 7. **Tensile test** (PA6 at 80 °C)

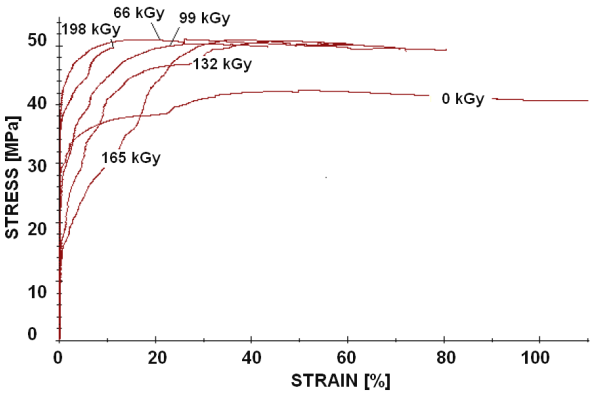

Fig. 8. **Tensile test** (PA6.6 at 80 °C)

Discussion

Generally said the irradiation of polyamides catalyzes the tensile strength and E modulus. Irradiation of PA6 (unfiled) bring improvement both the tensile strength and E modulus of about 22 % by the dose of 66 kGy, measured by room temperature (Fig. 9). Higher doses of irradiation are conductive to soft growth of value of ultimate tensile strength but the difference in these values with doses from 66 to 198 kGy is very low (max. 3 %). The value of E modulus drop with increasing doses of irradiation and the fall of E modulus reaches up to 11 %. By irradiation with the dose of 198 kGy is this property of about 10 % higher than in case of not irradiated polymer (Fig. 10). In case of not filled PA6.6 the irradiation gives only small improvement of tensile strength. Maximum value is reached by the dose of 132 kGy and after that it sinks.

The same tendency is remarkable also by E modulus. The increases of ultimate tensile strength of PA 6 filled by 30 % of glass fibres reaches cca 8 % and do not change with the doses of irradiation. The improvement of E modulus after irradiation with the dose of 66 kGy changes the reinforced PA6. The of E modulus of reinforced PA6 after irradiation with the dose of 66 kGy reaches to 23 % and there is a dorp of

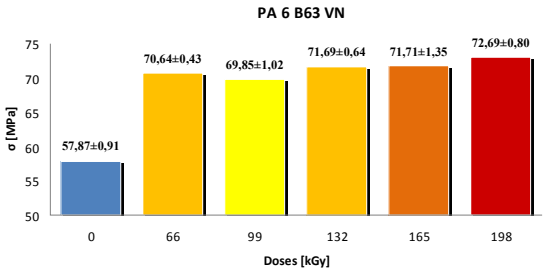

Fig. 9. **Tensile test** (PA6 at 23 °C)

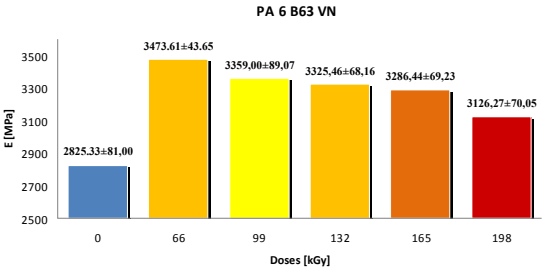

Fig. 10. **E modulus** (PA6 at 23 °C)

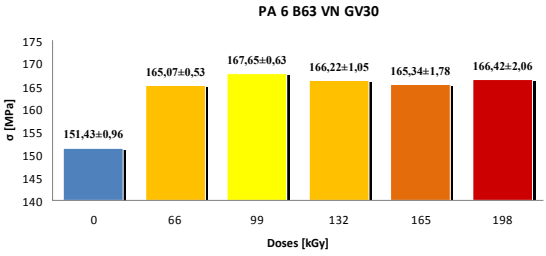

Fig. 11. **Tensile test** (PA6.6, 30 GF at 23 °C)

E up to 10 % bellow the value of not irradiated polymer. The ultimate tensile strength of reinforced PA6.6 will be improved by irradiation of about 10 % and it is going up with the higher dose of radiation. The growth of E modulus is marked already by the doses of 66 kGy and it is going up with the higher dose of irradiation.

By the temperature of 80 °C the ultimate tensile strength grows of about 7 % by PA6 and 15 % by PA6.6. Further increasing of dose of irradiation brings no changes. E modulus rises of 21 % (PA6) respectively 44 % (PA6.6). With growing dose of irradiation the E modulus does not change. The growth of ultimate tensile strength of PA6 and PA6.6 filled by 30 % of glass fibres reaches 7 % (PA 6) resp. 13 % (PA6.6) and is going up with the dose of irradiation. The same tendency is remarkable in case of E modulus.

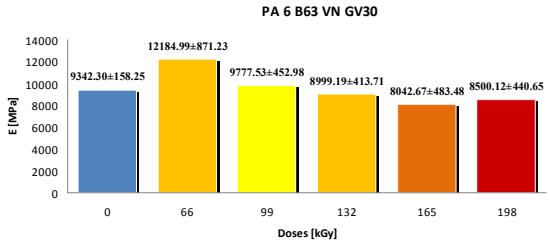

Fig. 12. **E moduilud** (PA6.6, 30 GF at 23 °C)

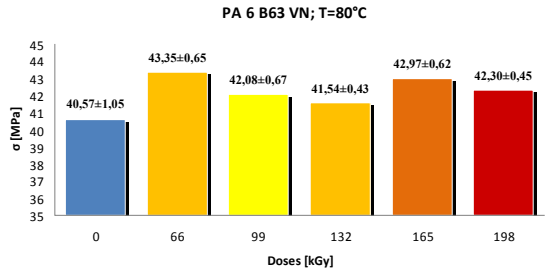

Fig. 13. **Tensile test** (PA6 at 80 °C)

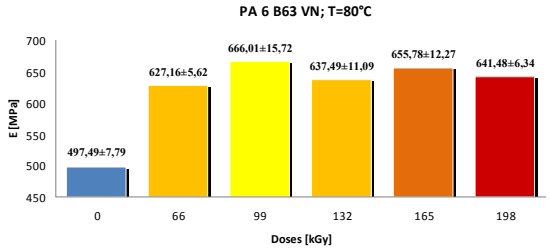

Fig. 14. **E modulus** (PA6 at 80 °C)

Conclusion

Irradiation improves mechanical properties of filled an unfilled PA6 and PA6.6. Substantial improvement was found already by the dose of irradiation 66 kGy. Higher doses have only limited effect on the follow up properties.

This article is financially supported by the Czech Ministry of Education, Youth and Sports in the R&D project under the title 'Modelling and Control of Processing Procedures of Natural and Synthetic Polymers', No. MSM 7088352102.

REFERENCES

1. Zyball A.: *Strahlungsenergie zur Modification von Kunststoffen – Industrielle Anwendungen der Bestrahlungstechnik*. In: Strahlenvernetzte Kunstoffe, Springer Verlag, Dusseldorf 2006.
2. Drobný J. G.: *Radiation Technology for Polymers*. CRC Press, Boca Raton 2003.

KL-11
THE RELATION BETWEEN MECHANICAL AND THERMAL PROPERTIES OF POLYPROPYLENE FIBRES

ANTON MARCINČIN*,MARCELA HRICOVÁ, KONŠTANTÍN MARCINČIN, and ALENA HOFERÍKOVÁ

Slovak University of Technology in Bratislava, FCHFT, IPM, Department of Fibres and Textile Chemistry, Radlinského 9, 812 37 Bratislava, SK
anton.marcincin@stuba.sk

A relation between mechanical properties and structure of polymers is permanently actual mainly from the point of view of development of tailored polymeric materials[1,2], including textile and technical fibres[3]. The effect of structure on mechanical properties is very actual for characterization of the classical and new developed fibres based on polypropylene produced from Ziegler-Natta (zniPP) and metallocene (miPP) catalyzed processes. The melt spinning of miPP and standard zniPP to compare processing of both kinds of PP and selected properties of fibres was studied by E. B. Bond, J. E. Spruiell and others[4–8]. The effect of the spinning speed on the density of fibres, crystallinity, crystalline and non-crystalline orientation functions, was investigated. The mechanical properties of fibres were explained on the basis of the nature and orientation of noncrystalline portions. The impact of orientation of PP composite fibres on their thermal and mechanical properties was studied also in our previous research[9].

In this paper, the spinning and selected mechanical and thermal properties of PP fibres were studied. The two kinds of the equivalents of commercial miPP and conventional-based zniPP were used in experimental work. Both zniPP and miPP resins were spun at the same spinning conditions within the 190–290 °C. The thermal and mechanical properties of zniPP and miPP fibres are presented and correlated in the paper as well

Experimental

Materials and procedure used

a) Ziegle-Natta isotactic polypropylene (zniPP) PP Moplen 561R (PP561R), MFR 25 g/10 min and PP Moplen HP561N (PP561N), MFR 11 g/10 min,

b) Metallocene isotactic polypropylene (miPP) PP Moplen 562R (PP562R), MFR 25 g/10 min, PP Moplen HP562N

(PP562N), MFR 11 g/10 min and PP Moplen 562S (PP562S) MFR 30 g/10 min.

All PP resins are produced and delivered by Lyondel-Basell Polyolefins

Melt spinning of PP fibres

The laboratory single-screw extruder D = 16 mm, L/D = 30 and spinneret with 13 orifices, d = 0.5 mm. was used for melt spinning of fibre grade PP. The spinning temperature was within 190–290 °C. Metering of the melt was 15 g min^{-1}, spinning speed 210 m min^{-1}. Fibres were drawn using laboratory drawing machine at 120 °C for the scale of draw ratio up to maximum draw ratio.

Methods used

Rheological measurements: Rheological properties of PP and PP composites were measured using capillary extrusiometer Göttfert N 6967 with extruder ϕ = 20 mm at 190–290 °C. The diameter of capillary was 2 mm and length was 30 mm. The Newton and Oswald de Waele laws were used for calculation of basic rheological parameters: apparent viscosity $\eta = \tau/\gamma$ and power law index n ($\tau = k.\gamma^{\cdot n}$), where τ-shear stress, γ – shear rate, η – apparent viscosity, n – power law index, k – coefficient.

Mechanical properties of the blend fibres: The Instron (Type 3343) was used for the measurements of the mechanical properties of fibres (according to ISO 2062:1993).

DSC measurements: The measurements were performed using Perkin Elmer DSC 7 in the temperature range 30–200 °C. The standard heating rate was 10 °C min^{-1}. The measurements were carried out using classic method (CM) and constant length method (CLM) in which the fibres with constant length during measurement were assured. The melting peak temperature T_p and melting enthalpy ΔH_m were evaluated.

Results and discussion

Rheological properties of PP resins

The melt viscosity and deviation from the Newtonian behaviour, expressed by power law exponent n are very similar for zniPP and miPP resins (Fig. 1 and Table I).

In general, the results of rheological measurements reveal that melt viscosity of miPP is moderately higher in average in comparison with zniPP equivalent. The difference is higher for couple with lower MFR. of PP. In spite of higher viscosity, mentioned miPP exhibited lower deviation from the Newtonian behaviour. The lowest deviation from the Newtonian flow is characteristic mainly for miPP562S from the tested polymers.

Table I
The power law exponent n and viscosity η for the selected shear rate for PP at various temperatures

PP/T [°C]		n	η [Pa s] γ =100 [s^{-1}]
PP 561R	230	0.44	327
	250	0.48	261
	280	0.50	195
PP 561N	230	0.39	476
	250	0.43	400
	280	0.44	314
PP 562R	190	0.39	550
	230	0.46	357
	250	0.49	289
	280	0.61	177
PP 562N	230	0.42	511
	250	0.45	426
	280	0.55	295
PP 562S	190	0.40	493
	230	0.52	284
	250	0.57	217
	280	0.65	146

Mechanical properties of PP fibres

The basic mechanical properties of the examined zniPP and miPP fibres spun at the various temperatures and cold

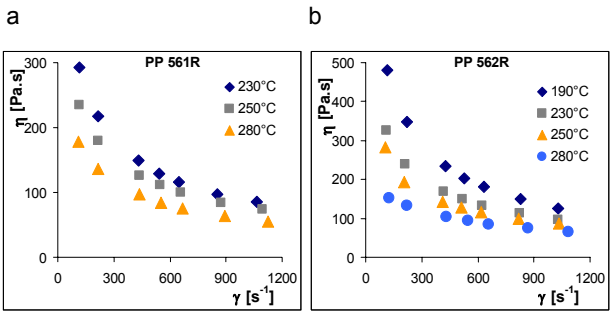

Fig. 1. **Dependences of dynamic viscosity on shear rate for zniPP561R (a) and miPP562R (b) at various temperatures**

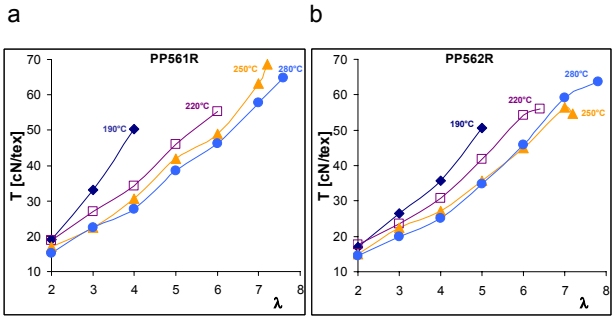

Fig. 2. **Dependence of the tenacity T on draw ratio λ for PP fibres spun at various spinning temperature. a. PP561R, b. PP562R, c. PP562S**

Table II
Tenacity T and Young's modulus YM for zniPP and miPP fibres spun at the temperatures 220 °C and 280 °C for constant elongation of fibres E = 20 % and E = 35 %

Sample		220 °C		280 °C	
		T [cN/tex]	YM [N/tex]	T [cN/tex]	YM [N/tex]
E 20 %	PP561R	54.0	6.88	58.4	7.98
	PP562R	54.0*	7.50*	54.1	7.56
	PP561N	42.0*	4.90*	53.2*	7.55*
	PP562N	56.0*	6.50*	59.3	7.46
	PP562S	57.6	8.10	50.5	7.87
E 35 %	PP561R	34.5	4.02	43.1	6.16
	PP562R	46.5	5.82	38.0	5.07
	PP561N	41.2	4.39	45.3	5.76
	PP562N	41.9	4.88	44.0	5.48
	PP562S	43.4	5.82	34.4	4.86

* extrapolated values

drawn are presented on the Fig. 2. The dependences on the Fig. 2 give information regarding the effect of drawing on tenacity of conventional and metallocene PP fibres spun at various spinning temperatures within 190–290 °C. The negative effect of the low spinning temperature (190–220 °C) on tenacity of fibres was found for zniPP561N and zniPP561R. The less sensitive resins to low spinning temperature were miPP562R and miPP562N. The spinning temperature 220 °C without any negative effect on tenacity of fibres was found for miPP562S. The high tenacity of fibres based on all investigated resins was obtained at high spinning temperature (280–290 °C).

To compare the mechanical properties of zniPP and miPP spun within the spinning temperatures of 190–290 °C and drawn at the same conditions, the tenacity and Young's modulus of the fibres were calculated and extrapolated for constant elongation E = 20 % and for E = 35 % (Table II).

The results reveal that the highest tenacity and Young's modulus of fibres for elongation of 20 %, were obtained for zniPP561R and miPP562N, both spun at 250 °C. The fibres are suitable for technical (industrial) textiles. The highest tenacity and Young's modulus of fibres for elongation of 35 %, were found for zniPP561N, spun at 250 °C and 280 °C and for miPP562N, spun at 280 °C. The fibres are suitable for common textiles when higher tenacity and elastic modulus are required.

Thermal properties of PP fibres

The DSC measurements were carried out using classic method (CM) and constant length method (CLM) at which the constant length fibres during measurement were assured. The results of thermal measurements of the zniPP561N as well as for miPP562N and miPP562S are given in the Tables III and IV. The DSC CLM method provides thermograms with different shape for fibres of different nature, MFR and also for fibres spun at various temperatures. Besides, the peak temperature increases with draw ratio (orientation) of fibres what is important result of DSC CLM method.

Table III
The peak melting point T_p and melting enthalpy ΔH_m for PP fibres spun at 220 °C and 280 °C, for various draw ratio λ, obtained using DSC CM method

PP	220 °C			280 °C		
	draw ratio λ	T_p [°C]	ΔHm [J g^{-1}]	draw ratio λ	T_p [°C]	ΔH [J g^{-1}]
PP 561N	1	162.6	80.6	1	161.5	77.2
	4.3	162.8	92.4	6	163.3	90.5
PP 562N	1	144.3	62.5	1	143.8	62.9
	5	144.5	81.1	6.8	147.0	76.9
PP 562S	1	144.5	59.8	1	143.8	63.2
	7.2	146.8	81.9	7.2	146.0	77.4

Both, melting temperature and melting enthalpy increase with higher draw ratio (orientation) of fibres. According to expectation, the metallocene resins provide lower melting temperature, especially miPP562S and lower melting enthalpy in comparison with zniPP561N (Table IV). The lower melting enthalpy of indicates the lower crystallinity of miPP compared to zniPP equivalent.

The gradually increase of the melting temperatures of both conventional and metallocene PP in dependence on draw

Table IV
The peak melting temperature T_p and melting enthalpy ΔH_m for PP fibres spun at 220 °C and 280 °, for various draw ratio λ, obtained using DSC CLM method

PP	220 °C			280 °C		
	draw ratio λ	T_p [°C]	ΔHm [J g^{-1}]	draw ratio λ	T_p [°C]	ΔH [J g^{-1}]
PP 561N	3	169.6	87.7	3	167.3	80.8
	4	182.1	85.8	5	179.2	85.3
	4.1	188.0	90.6	5.5	183.8	93.0
	4.3	184.0	86.3	6	185.2	91.7
PP 562N	3	157.0	68.8	3	151.3	68.2
	4	168.2	76.6	5	168.5	77.8
	4.7	173.0	77.2	6	173.5	77.4
	5	180.3	72.5	6.8	176.0	84.2
PP 562S	3	149.0	68.3	3	147.0	61.0
	5	156.5	77.7	5	154.2	76.7
	6	160.1	80.4	6	159.8	78.9
	6.5	161.8	83.6	7	165.6	86.9
	7.2	166.6	85.1	6.8	165.3	83.1
	7.5	169.2	85.4	7.2	165.5	86.2

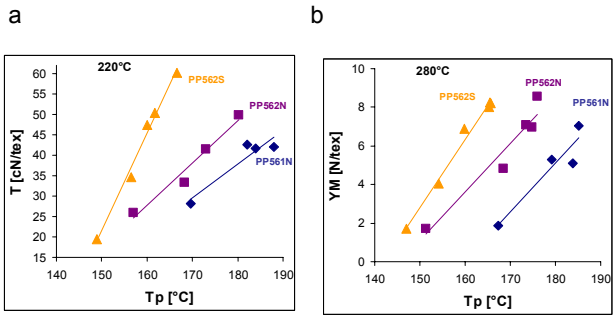

Fig. 3. **Dependence of tenacity T (a) and Young's modulus YM (b) on melting (peak) temperature T_p of PP fibres.** The multifilaments were drawn at draw ratio within2–7

ratio (orientation of fibres) results probably from increase of the total crystallinity of fibres and the higher height of crystals which grows in the fibres under tension at the relative high temperature in DSC pan. From this point of view, the increase of melting temperature of oriented fibres can result from the molecular orientation of fibres and can be correlated with their tensile properties such as tenacity or Young's modulus.

Correlation of the mechanical and thermal properties of PP fibres

Correlations of the tenacity and Young's modulus of fibres spun at 220 °C and 280 °C on their melting (peak) temperature are on the Fig. 3. The same correlations for tenacity and Young's modulus on melting temperature for fibres spun within the 190–290 °C were found. The correlations reveal that there is unambiguous straight-line dependence between tenacity and melting (peak) temperature as well as between Young's modulus and melting (peak) temperature of fibres, both obtained by DSC CLM method. These dependences were found for fibres based on both zniPP and miPP resins. The similar dependences but not such clear were obtained for tensile properties and melting enthalpy of fibres.

In the any case the melting (peak) temperatures of oriented PP fibres, obtained by DSC CLM method provide important information regarding the average orientation of fibres. Further analysis can give an answer on correlation of this melting temperature values with molecular orientation of fibres.

Conclusions

The following points of conclusion can be drawn:

The melt viscosity of miPP is moderately higher in average in comparison with zniPP equivalents. In spite of higher viscosity, miPP exhibited lower deviation from the Newtonian behaviour.

The DSC CLM method provides thermograms with different shape for fibres of different nature, MFR and also for fibres spun at various temperatures. Besides, the peak temperature increases with draw ratio (orientation) of fibres.

The unambiguous straight-line dependences between tenacity and melting (peak) temperature as well as between Young's modulus and melting (peak) temperature of miPP and zniPP fibres, obtained by DSC CLM method, were found.

Based on experimental results, from the point of view of the basic mechanical properties of miPP fibres and their zniPP equivalents there is not possible to prefer unambiguously conventional or metallocene PP. The advantages of higher deformability of miPP fibres could appear at higher spinning speed.

Experimental works were supported by Slovak Grant Agencies: APVV 0226-06 and VEGA 1/4456/07.

REFERENCES

1. Meijer H. E. H., Govaert L. E.: Prog. Polym. Sci. *30*, 915 (2005).
2. Boger A., Heise B., Troll C., Marti O., Rieger B.: Eur. Polym. J. *43*, 634 (2007).
3. Gregor-Svetec D., Sluga F.: Jour. Appl. Polym. Sci. 98, 1 (2005).
4. Misra S., Lu F. M., Spruiell J. E., Richeson G. C.: J. Appl. Polym. Sci. *56*, 761 (1995).
5. Andreasen E., Myhre O. J., Hinrichsen E. L., Gronstad K.: J. Appl. Polym. Sci. *57*, 1075 (1995).
6. Sundell T., Fagerholm H., Crozier H.: Polymer *37*, 3227 (1996).
7. Spruiell J. E., Lu F. M., Ding Z., Richeson G. C.: J. Appl. Polym. Sci. *62*, 1965 (1996).
8. Bond E. B., Spruiell J. E.: J. Appl. Polym. Sci. *82*, 3237 (2001).
9. Marcinčin A., Hricová M., Marcinčin K., Hoferíková A., Legéň J.: Fibres & Textiles in EE *15*, 64 (2007).

KL-12
VALORISATION OF WAST TYRE MATERIAL

WANDA PARASIEWICZ, MAREK TULIK, and JAN MĘŻYŃSKI

IMPIB Elastomers& Rubber Technology Div.
Ul. Harcerska 30; 05-820 Piastow
w.parasiewicz@impib.pl

Over a billion tires are sold worldwide each year and subsequently just as many fall into the category of end-of-life tires. European Landfill of the Waste Directive from 1999 introduced a ban of the landfills of used tires (since 2003) and shredded tires (2006). It was the obligation of member countries to create the proper legislation for implementation to the Directive. The key point was the acceptance of the 'Producer Responsibility' strategy. It created the challenge for producers and users of tires to develop efficient ways for end-of-life tires recovery. Material recycling is the one of more preferable methods of recovery of the valuable material. The results of this activity are shown by the data of different ways of recovery.

In 2006, there were approximately 3.2 million tons of used tires in the enlarged Europe. For the EU-15 alone, the annual volume increased from 2.1 million tons in 1994 to 2.7

million tons in 2006. However, in the same time frame, the EU's total recovery rate rose from 38 % to 87 **%**. This positive achievement clearly demonstrates that end-of-life tires are being sustainably diverted from landfills. The major markets benefiting from this are the material recycling (34 %) and energy recovery (32 %) sectors, which show that the market for end-of-life tire-derived products has become sustainable and economically viable. Encouraging results in 2007 are close to 90 % of ELTs in Europe are recovered[1].

The first step of tire recycling is size reduction, usually by grinding. Rubber crumb of different sizes received in such kind of processes have limited the area of application, because its admixing to new rubber compounds result in a significant drop of mechanical properties[2]. The next stage of process is the valorisation, which allows obtaining new rubber material with satisfactory properties.

Many ways the valorisation of rubber crumbs exist now but only a few are commercialized. The most popular since the late 90's have surface modification of rubber granules, like Sucrum introduced by Vredestin[3],or De – Link[4] or modification with functionalized polymers[5].

Another way of upgrading the material is by devulcanization commercialized as reclaiming. This is the process of cleaving the monosulfidic, disulfidic, and polysulfidic crosslinks of vulcanized rubber, without cleavage of polymer chains. The product can be re-vulcanized/re-cured to form new rubber articles.

In practice, a pure devulcanization process is very difficult to achieve since many problems are caused by accompanying chemical transitions such as depolymerization, thermal destruction and oxidation, which worsen the properties of the recovered elastomers.

The main problem hampering the appropriate running of the devulcanization process is the very low thermal conductivity of rubber resulted, an extremely difficult selective regulation of the quantity of energy carried to the cross-linking bonds.

Theoretically, the energy input should be sufficient for the dissociation of the S-S bonds (271.7 kJ mol^{-1}) and C-S bonds (301 kJ mol^{-1}), but at the same time too low for dissociation of the C-C bonds (347 kJ mol^{-1}) of the polymer chains. In practice, it's virtually impossible to achieve such an exact level of energy evenly distributed within the material. It's necessary to experimentally find the optimal devulcanization process and conditions, under which devulcanized products with good properties can be obtained.

One of the oldest and simplest devulcanization methods in the rubber reclaiming industry is called the ''pan process''[6].

In this process, finely ground rubber powder mixed with oils and devulcanizing agents are heated with steam in a pressure vessel at a temperature of ca. 200 °C for more than 5 h. Moreover, this process must usually be followed by several procedures (refining and straining) for obtaining the final devulcanized rubber. The devulcanized rubber obtained by this method is much more inferior in physical properties to a virgin (new) rubber, due to the occurrence of breakages of both the crosslinking points and main chain (C–C) bonds unselectively.

Hence, new material recycling technologies such as microwave devulcanization[7,8] and ultrasonic devulcanization[9] methods have been developed with the aim of shorter reaction times and optimizing the parameters in the reactor such as shear stress, temperature, pressure[6]. However, the devulcanized rubber obtained by these methods still was not good enough in quality to be widely applicable in practical use.

The new approach is continuous devulcanization performed on a modular twin screw extruder.

In the first zone of this process, roughly crashed rubber material is made into fine particles by high shearing and heating to the devulcanization-reaction temperature quickly. The principle of this method is the difference of the elastic constant for -C-C- and the crosslinking sulfur bonds, estimated to be 1/30 of C-C bonds[10]. This phenomena is responsible for the selective cleavage in a high shear condition in the extruder. The residence time is assured to be enough to complete the devulcanization reaction under the shear flow in the next zone. In this reaction zone, the fine particles of the vulcanized rubber become highly elongated by filling and shearing with the kneading disk elements, and thus eventually result in plasticizes of devulcanized rubber. After the process, the devulcanized rubber is extruded from the head of the reactor and cooled in the water bath.

The result of the process depends on the feeding rate, design of screws and temperature distribution along the extruder. The proper optimization of these parameters is the key for the good properties of received material.

The efficiency of devulcanization could be improved by admixing the peptizer and or reclaiming agent which accelerate the process. The most common reclaiming agents are disulfides, e.g. aryl disulfides such as diphenyldisulfide, thiophenols and their zinc salts and mercaptanes. These compounds are radical scavengers; they react with the radicals generated by chain or crosslink scission and prevent recombination of the molecules.

In the frame of this project the optimization of processing parameters in specially designed twin screw extruder was performed.

The extruder with co-rotating screws 40 mm diameter L/D 39 with 7 heating zones with max. screw speed 500 rpm was used to devulcanize buffing rubber material with an output 80 kg hr^{-1}.

The devulcanized material obtained shows Mooney plasticity 50+/−5 ML(1+4)×100, and tensile strength in the range of 10–12 MPa.

The 20 phr of this material was admixed to tread tire compound used for retreading truck tires. The experimental tires are actually tested.

The overview of the valorization methods of tire material and experimental trials made with the use of a prototype of the twin screw extruder made in IMPIB confirm that it is a promising way of the valorization of tire rubber granulate and to open the possibility of up-scaling the technology.

The overview of the valorization methods of tire material and experimental trials made with the use of a prototype of the twin screw extruder made in IMPIB confirm that it is a promising way of the valorization of tire rubber granulate and to open the possibility of up-scaling the technology

The work is financially supported by Polish Ministry of Science and Higher Educations the Research Project nr R08 029 03 carry out in the years2007-2010.

REFERENCES
1. Cineralp F.: ETRMA Report, "End of life tyres-avaluable 117 resorce with growing potential" 2007 Edition.
2. Pysklo L., Parasiewicz W., Stępkowski R.: Elastomery *4*, 15 2 (2000).
3. Dirkes W.:Elastomery *3*, 18 (1999).
4. Parasiewicz W., Pysklo L., Wilkonski P.: A New simple method of mechanochemical devulcanization of rubber wastes. *Conference proceedings, Polymers-Environment-Recycling, Szczecin-September 1995*.
5. Parasiewicz W., Stępkowski R., Ostaszewska U., Tulik M.: Elastomery *10*, 14 (2006).
6. Myhre M., Mackillop D. A: Rubber Chem. Technol. *75*, 429 (2002).
7. Novotony D. S.: Microwave devulcanization of rubber, US Patent 4,104,205, 1978.
8. Parasiewicz W., Adamski W., Kleps T., Stępkowski R.: Elastomery *2*, 23 (1998).
9. Isayev A. I., Tukachinsky A.: Rubber Chem. Technol. *68*, 267 (1995).
10. Fukumori K., Matsushita M.: Tech. J. R&D Rev. of Toyota *38*, 39 (2003).

KL-13
SHAPE-MEMORY BEHAVIOR OF PEROXIDIC CROSS-LINKED POLYETHYLENE BASED BLENDS

HANS-JOACHIM RADUSCH and IGOR KOLESOV

Martin Luther University Halle-Wittenberg, Chair of Polymer Technolog,y, D-06099 Halle, Germany
hans-joachim.radusch@iw.uni-halle.de

Abstract

Shape-memory (SM) polymers are characterized by a specific temperature and load controlled deformation behavior. They can be advantageously used e.g. in cable and packaging industry, medicine or automotive. Precondition for proper appearance of the thermal induced SM effect (SME) is the existence of stable physical or covalent molecular network and glass or phase transition, respectively, at relevant temperatures.

The thermally induced SME of binary and ternary peroxidic cross-linked blends from several ethylene-1-octene copolymers (EOC) and/or nearly linear polyethylene (HDPE) was investigated. The SME behavior of the prepared materials was evaluated by the characteristic parameters strain recovery (R_t), strain fixity ratio (R_f) and SM recovery rate ($d\varepsilon(T)/dt$) in dependence on programming conditions.

It was found that triple and quadruple SME could be observed after two- and accordingly three-step programming of binary and ternary HDPE/EOC blends, respectively, at suitable temperatures and durations. The effects correlate with multiple melting/crystallization behavior of HDPE/EOC blends.

Introduction

For covalent (e.g. peroxidic) cross-linked semi-crystalline polymers the SM behavior with high performance can be achieved, firstly, if this polymeric material possesses a resistant network with suitable high cross-link density and as a consequence of this produces sufficiently large elastic and viscoelastic forces under load at programming temperature $T_{pr} > T_{trans}$ and preferably lowest residual strain as well as shows high enough break strain, and secondly if its crystalline phase formed after cooling of the programmed (loaded) sample is able to fix efficiently the strain and elastic and viscoelastic forces stored in the network. The ability of SM polymers to strain fixation and to form regeneration is characterized by strain fixity (R_f) and strain recovery ratios (R_r), respectively, which are defined according to Lendlein and Kelch[1] as:

$$R_f = \frac{\varepsilon_v}{\varepsilon_{pr}}, \qquad R_r = \frac{\varepsilon_{pr} - \varepsilon_{rec,m}}{\varepsilon_{pr}} \qquad (1)$$

where ε_{pr} is the strain caused by programming, ε_v is the strain that remains after programming, cooling, unloading and recovery at lowest temperature of experiment of specimen and $\varepsilon_{rec,m}$ is the residual strain that resides after thermal-induced recovery (shrinkage) at maximum temperature of experiment. The objective of the presented work was the production of peroxidic cross-linked binary and ternary blends on the basis of HDPE and two EOCs with medium and high degree of branching as well as the investigation on their multiple SM behavior and their characterization by the relevant thermal and mechanical properties.

Experimental

Polyethylenes used were HDPE (KS 10100 UE) and EOCs (AFFINITY TM PL 1280G and ENGAGE 8200) (Dow Chemical) with 30 and 60 hexyl branches per 1000 C (EOC30 and EOC60). As cross-linking agent 2,5-dimethyl-2,5-di-(*tert*.butylperoxy)-hexane (DHBP) (Degussa) was used. The mechanical mixes of DHBP impregnated polymer pellets in desired ratio (Table I) were blended by a single-screw mixing extruder (Brabender) at 130 °C. As reference object a HDPE was prepared in the same manner.

Designation	HDPE [%]	EOC30 [%]	EOC60 [%]
100HDPE	100	–	–
50HDPE/50EOC30	50	50	–
33HDPE/33EOC30/34EOC60	33	33	34
10HDPE/45EOC30/45EOC60	10	45	45
10HDPE/25EOC30/65EOC60	10	25	65
50EOC30/50EOC60	–	50	50
30EOC30/70EOC60	–	30	70

The extrudates were processed to 1 and 2 mm films at 140 °C and cross-linked at 190 °C. The tensile tests in the

temperature range of SM tests programming (120 and 140 °C) has been carried out using a testing machine Zwick 1425 (Zwick) with heating chamber and a load cell 10 N at a crosshead speed of 50 mm min^{-1}. Test bars were used with the cross-section area 2.0×2.0 mm^2. Thermal analysis was performed by DSC 820 (Mettler-Toledo) at a heating and cooling rate of 20 and 10 K min^{-1}, respectively. For the characterization of the shape memory behavior the samples came at first under a specific temperature-deformation program. The samples were programmed at a stretching strain of $\varepsilon_{pi} \leq 100$ % during a dwell period of 120 s at the programming temperature T_{p1}, and cooled down to T_{p2} with an average cooling rate of approx. 11 K min^{-1} in a constant deformed state. Before loading of the next programming strain ε_{pi} the sample temperature was kept constant for 10 min. After last programming step the specimen was cooled down to 10 °C at the programming strain of 100 %, thermal equilibrated for 10 min and unloaded. The recovery strain was measured first after a delay of 10 min at 25 °C (ε_v) and than in the course of a heating run with a rate of 2 K min^{-1} and 'zero' stress of 70 Pa ($\varepsilon_{rec}(T)$). Complete SM investigations were carried out in tensile mode using a mechanical spectrometer measuring head Mark III (Rheometric Scientific).

Results and Discussion

From the results of stress-strain measurements and the Mooney-Rivlin equation as well as rubber elasticity theory the degree of cross-linking and average molar mass of the polymer chains between two neighboring network nodes were calculated. All investigated materials with the exception of HDPE evidence a small increase of ν_c and consequently decrease of $\bar{M}_c$ values at higher temperature. The ν_c values change not significantly and varies approx. from 110 to 140 mol m^{-3} at 120 °C and from 80 mol m^{-3} for HDPE as well as 150 to 170 mol m^{-3} for blends at 140 °C, respectively.

The melting and crystallization behavior of HDPE and HDPE/EOC30/EOC60 blends is displayed in Fig. 1.

Only second heating runs at a cooling rate of 10 K/min were used for the analysis of melting behavior. All blends demonstrate multiple behavior for both melting and crystallization (Fig. 1). In 10HDPE/45EOC30/ 45EOC60 and 10HDPE/25EOC30/ 65EOC60 blends the HDPE phase crystallizes at 97.7 °C and 100.3 °C, respectively. Moreover, the local cross-linking degree in the HDPE phase is by all means lower than the average cross-linking degree of the blend as a whole. Obviously, the described behavior of blends suggests the crystallization of the main part of HDPE phase together with the EOC30 at significantly lower temperature. Interestingly, the melting of the HDPE phase in 10HDPE/45EOC30/ 45EOC60 and 10HDPE/25EOC30/65EOC60 blends occurs also stepwise in two stages (see Fig. 1).

T_m and T_c of the HDPE phase decrease markedly with decreasing HDPE content in the blend compared to the values for 'bulk' cross-linked HDPE. At the same time, T_m and T_c values of the EOC30 phase can increase in blends containing HDPE or decrease in binary blends with high branched EOC60. In blends both nucleating effect of HDPE crystallites and molecular interaction are available only in uncross-linked crystalline domains which consist of ethylene sequences of blend components with suitable length. Due to the existence of several populations of PE crystallites of different stability and correspondingly with different melting temperatures in the described blends the thermograms in Fig. 1 show nearly continuous melting by that the SM behavior of these blends is affected.

The SM behavior and especially the temperature dependence of SM recovery strain and recovery strain rate of HDPE and HDPE/EOC30/EOC60 blends and their components having a network with similar cross-linking degree are demonstrated in Fig. 2. Here, the findings of the first cycle of SM tests are demonstrated. The sharp step of SM recovery strain and high, well separated peaks of SM recovery rate can be generated only by melting of a phase with sufficient crystallinity and relatively perfect crystallites.

For the explicit appearance of SME the availability of stored sufficiently high visco-elastic forces is important no less than suitable melting behavior. These visco-elastic forces caused by network deformation during programming must be efficiently stored by the crystalline structure formed in the actual temperature range. As expected, the blends having a higher average crystallinity exhibit the high strain fixity ratio R_f and SM recovery rate $-d\varepsilon_{rec}/dt$. Correspondingly, these parameters increase with increasing HDPE (and partly EOC30) content in the blends. The single-step programming of all blend types results in appearance of only one step and accordingly one peak in the temperature dependences of the SM recovery strain and SM recovery rate, respectively, i.e. in

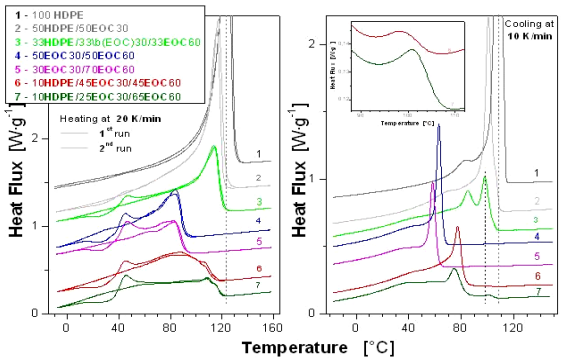

Fig. 1. **Melting (left) and crystallization (rigth) of cross-linked HDPE and HDPE/EOC blends**

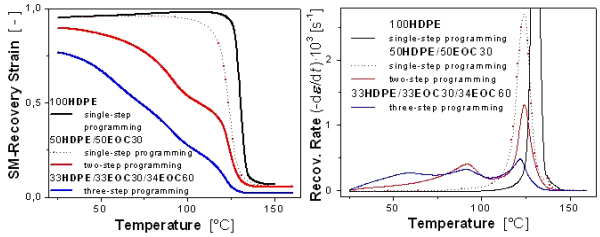

Fig. 2. **Effect of composition and programming conditions on the temperature dependence of SM recovery strain (left) and recovery strain rate (rigth) of HDPE and binary and ternary HDPE/EOC blends**

dual-shape behavior. The blends after two- or three-step programming show significantly lower R_f and $-d\varepsilon_{rec}/dt$ values and particularly $[-d\varepsilon_{rec}/dt]_{max}$ values at melting temperatures of the components (see Fig. 2). The decrease of R_f values as a result of multi-step programming is caused by the partial deformation of already crystallized (fixed) phase/phases by each next programming step at lower temperature. All investigated blends and their components independent from programming mode demonstrate relatively high values of strain recovery ratio (R_r) that amounts approx. 93 to 98 %. Presumably, the multi-shape behavior by single-step programming may be carried out only in a heterogeneous polymer material having a phase morphology with preferred orientation of planar phase layers perpendicularly to the load direction (Kolesov and Radusch[3]).

REFERENCES
1. Lendlein A., Kelch S.: Angew. Chem., Int. Ed. Engl. *41*, 2034 (2002).
2. Li F., Chen Y., Zhu W., Zhang X., Xu M.: Polymer *39*, 6929 (1998).
3. Kolesov I. S., Radusch H.-J.: eXPRESS Polymer Letters *2*, 461(2008).

KL-14
APPLICATION OF ALIPHATIC POLYAMIDES AS ENGINEERING PLASTICS

JAN RODA

Institute of Chemical Technology, Department of Polymers, Technická 5, CZ16628 Praha 6, Czech Republic
jan.roda@vscht.cz

KL-15
NEW ELASTOMER MATERIALS MADE OF ELASTOMER BLENDS MODIFIED BY SPECIFIC INTRA- OR INTERELASTOMER REACTIONS

WLADYSLAW M. RZYMSKI*, KINGA BOCIONG, and MAGDALENA KMIOTEK

Technical University of Lodz,Institute of Polymer & Dye Technology, 90-924 Lodz, Stefanowskiego 12/16, Poland
rzymski@p.lodz.pl

The lack of thermodynamic miscibility of the rubbers (A, B) causes that the crosslinking reactions in rubber blends occur mostly independently in the microphases of each component (in intermolecular, intraelastomer reactions in rubber A and B respect.) and – to some extent – in interelastomer crosslinking reactions, resulting in interelastomer crosslinks *X* between rubber A and B, *e.g.* in A-*X*-B structures. It is caused by the curing agent solubility in A and B, its reactivity to A and B, and by the existence of interphase layer of different thickness and structure[1].

However, epoxy groups of epoxidized natural rubber (ENR) react with ~SO_2-Cl groups of CSM (chlorosulfonated polyethylene), with ~CO-OH groups of XNBR (carboxylated nitrile) or with allyl Cl groups in chloroprene rubber (CR). It leads to interelastomer crosslinks in ENR-CSM, ENR-XNBR ENR-CR and CSM-XNBR blends, even if no curing agent was used (self-vulcanizable elastomer blends SVEB)[2,3]. However, curing of such blends needs long heating time and results in products of limited curing degree and of poor mechanical properties.

From the other side, selective, dynamic curing of a rubber (in intraelastomer reactions), connected with its dispersion during mixing with a selected plastomer, results in valuable engineering materials, thermed thermoplastic vulcanizates[4–6].

In our studies we found new cured, elastomer materials prepared from elastomer blends modified by the specific intra- and/or interelastomer reactions, governed by other factors than in the SVEB case.

Elastomer blends modified by specific intraelastomer reactions

Such modification occurs due to the neutrali-zation of ~CO-OH groups in XNBR with metal compounds during rubber dynamic curing and dispersion in other elastomer, followed by static (conventional) curing of the blend obtained. In our studies[7] hydrogenated nitrile rubber (HNBR, bound acrylonitrile content: 42.5 %; hydrogenation degree: 99 %) was modified with XNBR (bound acrylonitrile: 27 %; bound acid: 7 %). XNBR was dispersed in HNBR and cured with MgO during blend mixing in micromixer. To dynamically prepared blends DCP (dicumyl peroxide) was added on two roll mill and the blends were than compression moulded in press and cured. The properties of dynamically and conventionally (all ingredients mixed on two roll mill only) prepared blends were than compared.

The properties of the prepared blends depend on the XNBR/HNBR-ratio, mixing time, amount of MgO used for selective XNBR curing and on the DCP amount used for static curing.. The dynamically prepared HNBR/XNBR blends (80/20 wt./wt.) are heterogenous systems with continuous phase formed by HNBR, in that microsized droplets and rod-like particles of cured XNBR are dispersed. In blends prepared conventionally each of elastomers forms its own continuous phases (two co-continuous phase morphology). The dynamically cured blends exibit higher crosslinking degree and higher tensile strenth (12–15 MPa) but lower swelling (~10 vol.%) in hexane than prepared conventionally (~15 vol.%).

The rective mixing of HNBR/XNBR blends connected with dynamical curing of dispersed, cheaper XNBR lead to compounds showed the properties of cured HNBR. Similar results were obtained for NBR/HNBR blends in that NBR was selectively, dynamically cured with sulfur-system during its mixing with HNBR.

Elastomer blends modified by specific interelastomer reactions

Such blends consist elastomers that can be cured due to the action of *in situ* generated initiators or due to its specific activity to the elastomers.

Blends containing styrene-butadiene rubber

The reactivity of α-methylene groups and >C=C< bonds in the styrene-butadiene rubber (SBR) is used for its curing with sulfur containing systems. From the other side, phenyl rings in SBR can be alkylated by halides or olefines in the Friedel-Crafts' reaction catalyzed with Lewis acids. We found[8–10] that the SBR/CSM blends undergo curing, when heated in the presence of ZnO, SnO or Fe_2O_3. The curing rate and degree, and the properties of cured blends can be modified by the CSM/SBR-ratio, the kind of CSM added (bound Cl: 24, 29 or 43 wt.%, CSM24, CSM29 and CSM43 respectively) and by the amount and kind of metal oxide incorporated, Table I.

Table I
Selected properties of SBR/CSM/ZnO blends (85/15/0.90 by wt.) cured at 423 K for 50 min

CSM	$2C_1$ [MPa]	Q_v^T [vol.%]	TS_b [MPa]
CSM24	< 0.05	3180	1.62
CSM29	0.304	470	4.12
CSM43	0.334	424	7.25

$2C_1$ – Mooney-Rivlin elasticity constant; Q_v^T – equilibrium swelling degree in toluene; TS_b – tensile strength

The curing is a result of the alkylation of SBR phenyl rings by CSM chains (thus – CSM bonding on the SBR) and by SBR chains containing vinyl side groups. The curing reaction is catalyzed by $ZnCl_2$ (Lewis acid) generated *in situ* from ZnO and CSM. The heating of CSM with ZnO leads to no curing.

The decrease of absorption intensity at 1164 and 1352 cm^{-1} (~SO_2-Cl groups), at 1639 cm^{-1} (vinyl side groups of SBR) and the changes in IR-spectra at 1700–1940 cm^{-1} (substitution in phenyl rings), the content of the fraction soluble in 2-butanone and the bound Cl content in cured and purified SBR/CSM blends confirm the proposed curing mechanism.

Recent investigations[11] indicate that chlorinated butyl rubber can replace CSM in such blends.

Blends containing CSM and XNBR

XNBR/CSM blends are self-vulcanizable, but the reached curing degree and the mechanical properties of cured blends are poor. We found that the heating of such blends at T < 440 K, if they contain up to 40 wt.% of selected CSM, metal compound and stearic acid, leads to cured products of high curing degree and high tensile strength[12]. The content of soluble fraction, bond Cl content in cured and than purified samples and the IR analysis indicate that the curing reactions include hydrolysis of ~SO_2-Cl groups to ~SO_2-OH and neutralization of ~CO-OH + ~SO_2-OH groups by metal oxide. Intra- [^{X}R~CO-O$^{(-)(+)}$Me$^{(+)(-)}$O-CO~R^{X}] and interelastomer [^{X}R-CO-O$^{(-)(+)}$Me$^{(+)(-)}$O-SO_2-R^{CSM}] ionic crosslinks are formed (Table II); ^{X}R = XNBR, ^{CSM}R = CSM.

The extent of such curing and the properties of cured blends depend on the CSM amount and kind, and the amount and kind of metal compound used.

Table II
Selected properties of CSM35/XNBR blends cured with 12 phr MgO and 2 phr stearic acid at 433 K for 30 min

CSM/XNBR	100/0	40/60	20/80	0/100
S_{e100}, MPa	–	3.2	4.4	5.5
TS_b, MPa	–	23.0	30.2	41.7
E_b, %	–	610	565	550
$2C_1$, MPa	–	0.37	0.34	0.35
Q_v^M, vol. %	∞	550	470	395
Cl^b, wt. %	–	7.4	7.6	0
S^M, wt. %	100	11	5	4

S_{e100} – stress at 100 % elongation; TS_b – tensile strength; E_b – elongation at break; $2C_1$ – Mooney-Rivlin elasticity constant; Q_v^M – volume swelling in 2-butanone, Cl^b – bound Cl content in samples extracted with 2-butanone; S^M – fraction soluble in 2-butanone

Summary

The proposed new curing method of the blends makes it possible to prepare new elastomer materials of interesting properties. The properties of such blends can be further modified with the reinforcing fillers or with the selected plastificators.

REFERENCES

1. Corish P. J., in: (Mark J. E., Erman B., Eirich F. R., ed.): *Science and Technology of Rubber*, Elastomer Blends, Chapter 12, p. 545, 2nd Edition. Academic Press, San Diego 1994.
2. Antony P., De S. K., van Duin M.: Rubber Chem. Technol. *74*, 376 (2001).
3. Rzymski W. M.: Polimery *39*, 422 (1994).
4. Coran A. Y., in: (Mark J. E., Erman B., Eirich F. R., ed.): *Science and Technology of Rubber*, Vulcanization, Chapter 7, p. 339, 2nd Edition. Academic Press, San Diego 1994.
5. Radusch H.-J., Rzymski W. M.: Elastomery *5*, 11 (2001); *5*, 3 (2001).
6. Rzymski W. M., Radusch H.-J.: Polimery *47*, 229 (2002).
7. Bociong K., Rzymski W. M.: Elastomery *12*, 21 (2008); Polimery *in press.*
8. Rzymski W. M., Wolska B.: Polimery *48*, 520 (2003); *49*, 524 (2004); Gummi Fasern Kunstst. *58*, 518 (2005).
9. Rzymski W. M., Wolska B., Wawrzecka A.: Ann. Pol. Chem. Soc. *2*, 146 (2003).
10. Rzymski W. M., Wolska B., Wawrzecka A.: Polish Patent 198303 (2007).
11. Rzymski W. M., Bociong K., Gietka K.: Polish Patent Declaration P-385040 (2008).

12. Kozioł M., Rzymski W. M.: Ann. Pol. Chem. Soc. *3*, 1015 (2004); Polimery *50*, 587 (2005); *52*, 511 (2007).

KL-16
POLYMER ADDITIVES AS ONE OF THE KEY FACTORS OF SUCCESS OF PLASTICS IN AUTOMOTIVE APPLICATIONS

LEONID SMOLIAK

Division PA, Clariant International Ltd, Rothausstrasse, 61, CH-4132, Muttenz, Switzerland leonid.smoliak@clariant.com

Plastics are widely used for automotive applications due to their low weight, mechanical characteristics, corrosion resistance and large variety of other properties compared to metals and glass. The major plastic parts of a modern car are made from such plastics as Polypropylene (bumpers), Polyamide (elements in under hood), and Polycarbonate (transparent roofing elements, head and rear light elements).

Polymer materials are affected by such factors as heat and UV light which initiate their oxidative degradation. Such consequences of polymer degradation as polymer chain breakage (loss of mechanical properties) and color formation are ones of the most important limitations of plastics utilization's in the demanding automotive applications.

However, there are ways to prevent and inhibit the reactions of photo- and thermal oxidative degradation of polymer materials and therefore to enhance their utilization options and service life. The most important way is the utilization of polymer additives, in particular, thermal and light stabilizers for polymers.

Main classes of polymer stabilizers are Phenolic Antioxidants, Processing Stabilizers, Light stabilizers (HALS) and UV-absorbers. Each class works through its own mechanism (chemical or physical polymer protection), very often one can observe a synergism between different stabilizers[2].

Role and need for stabilization varies depending on polymer resin type and end application requirements. For example, a Polypropylene grade (general purpose or specific PP) is always stabilized by phenolic AO and processing stabilizer whereas Polycarbonate macromolecules are more stable by themselves and require stabilization in very specific applications.

We will study some examples how polymer additives contribute the final performance of plastics for automotive industry.

Polypropylene stabilization

Polypropylene can be used for car exterior parts (like bumpers), interior and under hood elements. An under hood application requires as a must a long term heat stability (high exploitation temperatures in the engine compartment), while exterior and interior elements require both light stability and some heat stability.

The most efficient way of long term heat stabilization (LTHS) of PP is a combination of high efficient phenolic antioxidant and thio-synergist, with such a formulation you can increase LTHS of PP in times. Thio-synergists (peroxide decomposers) is a group of thermal stabilizers which gives strong synergetic effect to phenolic antioxidants under long term heat treatment of PP. Scheme 2 illustrates the effect of thio-compound on LTHS of Polypropylene.

Thus, due to combination of proper phenolic antioxidant and thi-synergist, Polypropylene materials can work under long term heat exposure.

Another very important application of PP in automotive is such parts of car exterior as bumper elements. Requirements in terms of light stability are normally include at least five years outdoor stabilization (means no dramatic changes in mechanical properties and color). This light stabilization level can be obtained with utilization of proper light stabilizer, like substances of Hindered Amine Light Stabilizer (HALS) class. Typical compound of HALS chemistry is product known as HALS-770 (bis(2,2,6,6-tetramethyl-4-piperidyl) sebaceate) which is quite efficient for PP thick article like

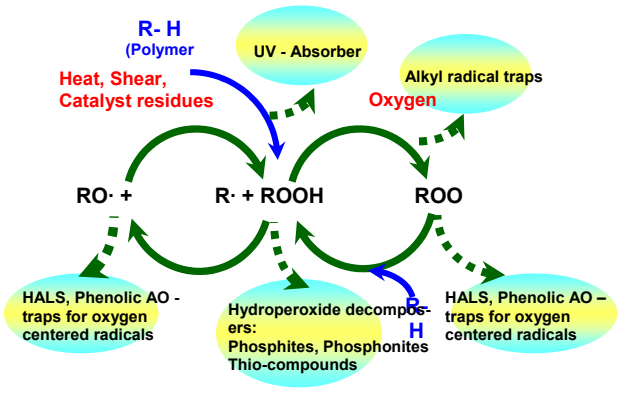

Scheme 1. **Mechanism of Polymer Stabilization**[1]

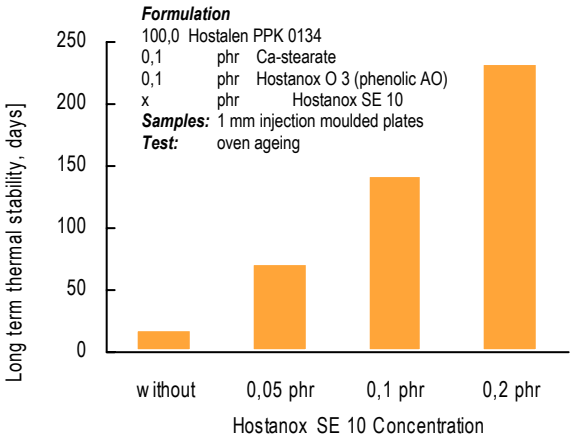

Scheme 2. **Enhancement of Long Term Thermal Stability of Polypropylene co-polymer with thio-synergist**

bumpers. However, there are secondary aspects of utilization of additives in polymers like poor solubility and diffusion of light stabilizers[3]. Solubility of HALS-770 additive in PP is on the level of tenths of a per cent which is exactly the level of effective concentration of HALS in PP for bumper application. Presence of HALS on its edge of solubility in PP creates so called physical effects (migration of the additive onto the surface) which lead to visible surface chalking. The 'state-of – the art' solution to this problem is the utilization of HALS with high solubility in PP matrix (such as Hostavin N845) or oligomeric HALS with low migration (such as Hostavin N30). Hostavin N845 has an excellent solubility (more than 3 %).

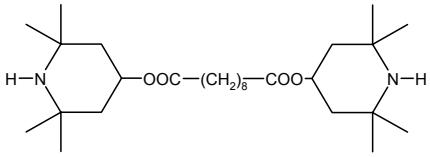

HALS-770 (bis(2,2,6,6,-tetramethyl-4-piperidyl)sebaceate)

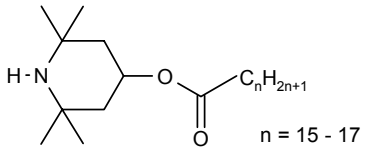

Hostavin N845

As one can observe from the Scheme 3, the higher solubility of Hostavin N845 is directly correlated to its efficiency at higher concentration, whereas Tinuvin 770 effect is limited by concentration of 0.3–0.5 %.

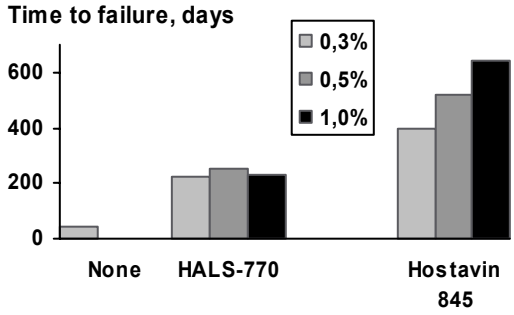

Scheme 3. **Comparison of low and high soluble HALS efficiency in PP.** Sample: EPDM Modified and Talc Filled PP; Test: Atlas WOM (DIN 53 357 A); Time to failure is calculated by visible chalking (increase of L value from 76 (original) to 80 or more)

Polyamide stabilization

Polyamide is widely used for glass-reinforced and filled engineering compounds for automotive parts (made by Injection Moulding) due to its higher mechanical properties, abrasion resistance and thermal stability. We can often find polyamide textile and technical yarns as a base material for safety belts, airbags and car seat covers. Polyamide tire cord is also one of the basic elements of a modern tire construction. Standard systems for thermal stabilization of Polyamides are copper based inorganic complexes (Copper Chloride based); these systems are quite efficient in terms of polymer protection. However, apart from efficiency in polymer, copper salts can give unfavorable discoloration of polyamide (green-blue shade) and they can be easily extracted since they are water-soluble. This is the first reason why polyamide industry looks for organic alternatives to Copper which are Phenolic Antioxidants. The second reason is the fact that for high demand applications of polyamide like automotive industry, there is a need for higher efficiency of stabilization of polyamide. Such a higher level of stabilization can be obtained with utilization of special stabilization agent like Nylostab S-EED ( ).

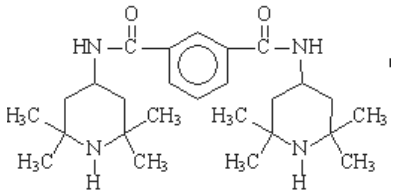

Nylostab S-EED

Nylostab S-EED can influence the processability, surface properties, heat and light stability of injection moulded parts and fibers (see Scheme 4 and 5).

Nylostab S-EED is a unique additive for polyamide which can be used during polymerization of Polyamide as well as during compounding and injection moulding processes. Apart from its excellent surface modification and filler dispersion aid effect, Nylostab S-EED work as a highly efficient light stabilizer for polyamides (because of its hindered amine structure). Best results of light stabilization (no color change) can be achieved by combination of Nylostab S-EED with a UV-absorber (Hostavin VSU).

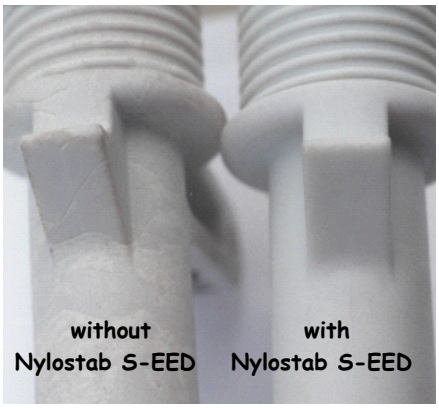

Scheme 4. **Surface modification of PA** (IM shaft) **by Nylostab S-EED** (additive of HALS class)

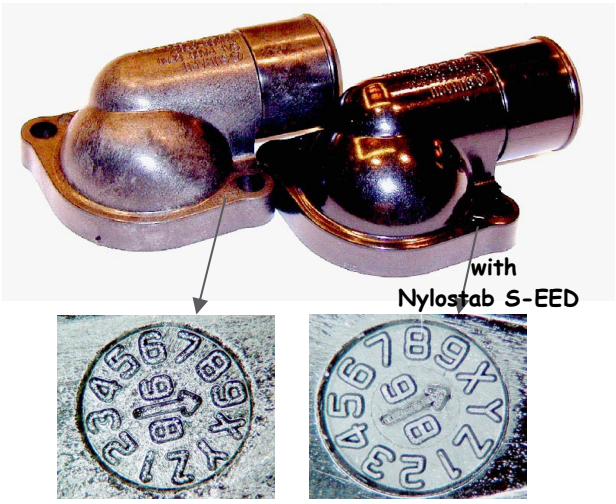

Scheme 5. **Surface quality of the Black Pigmented GF PA 6.6** (Circular marks on the molded parts)

Yellowness Index

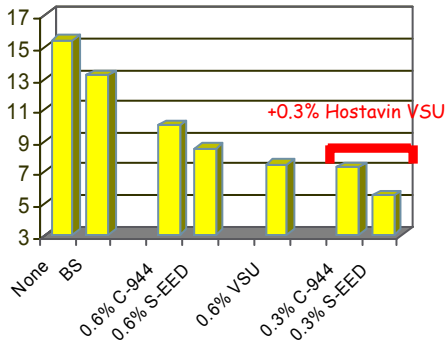

Scheme 6. **Light Stability of Polyamide** (Injection Moulding 1 mm plaques, Accelerated Weathering Conditions: 1500 hours in Atlas WOM (DIN 53 387 A)

Polycarbonate stabilization

A main application for Polycarbonate in automotive industry is a replacement of glass parts since Polycarbonate resin has excellent transparency and impact resistance. Stabilization of Polycarbonate articles is required for exterior parts of car like head lights and transparent roofs. A proper stabilization from UV light allows us to maintain mechanical properties and transparency of PC and the same time to prevent discoloration of PC which is essential for optical elements.

Conclusion

Automotive industry is a high demand application for polymer materials, utilization of polymer additives enables polymer producers to meet and overcome the specific requirements to plastic elements of cars such as long term heat stability and light stability.

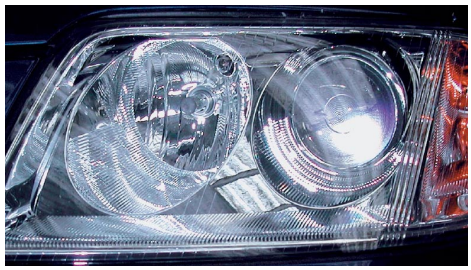

Scheme 7. **Head Light Element made from Polycarbonate requires high level of UV- and heat stabilization**

Stabilization is an essential and very often the only way to maintain mechanical, optical, aesthetical and other important characteristics of such plastics as PP, PA, PC, ABS during conditions of exploitation of a modern car.

REFERENCES

1. Zweifel H.: *Polymer Additives Handbook*, 5th edition, Hanser Gardner Publications (2001).
2. Malik J., Kröhnke C.: Comptes Rendus Chimie *9*, 1330 (2006).
3. Malik J., Hrivik A., Tomova E.: Polym. Degrad. Stab. *35*, 61 (1992).

KL-17
AUTOMOTIVE MATERIALS FROM PTS

WALTER BAUMANN

PTS Marketing- & Vertriebs-GmbH
Hautschenmühle 3
D-91587 Adelshofen-Tauberzell

1. Supertough glass fibre reinforced PP
PP + glass fibre is standard for automotive interior structural parts. The limit is dimension stability, impact and warping combined with not sufficient surface quality. Therefore PTS Group has developed a wide range of special compounds with super impact, good dimension stability and excellent surface.

2. Semi-aromatic highly glass reinforced polyamide for metal replacement
These special PA grades with typically 50-60 % glass fibre show excellent aesthetical surface, high impact and ultraflow properties for thin-wall-applications.

3. Cross-linkable polymers
With cross-linkable PA, PBT and other semi-crystalline materials, the gap between engineering plastics and expensive special polymers can be filled.